

The Risk Premia Embedded in Index Options[☆]

Torben G. Andersen^a, Nicola Fusari^{b,*}, Viktor Todorov^a

^a*Department of Finance, Kellogg School of Management, Northwestern University, Evanston, IL 60208*

^b*The Johns Hopkins University Carey Business School, Baltimore, MD 21202*

Abstract

We study the dynamic relation between market risks and risk premia using time series of index option surfaces. We find that priced left tail risk cannot be spanned by market volatility (and its components) and introduce a new tail factor. This tail factor has no incremental predictive power for future volatility and jump risks, beyond current and past volatility, but is critical in predicting future market equity and variance risk premia. Our findings suggest a wide wedge between the dynamics of market risks and their compensation, with the latter typically displaying a far more persistent reaction following market crises.

Keywords: Option Pricing, Risk Premia, Jumps, Stochastic Volatility, Return Predictability, Risk Aversion, Extreme Events.

JEL classification: C51, C52, G12.

[☆]Andersen gratefully acknowledges support from CREATES, Center for Research in Econometric Analysis of Time Series (DNR78), funded by the Danish National Research Foundation. Todorov's work was partially supported by NSF Grant SES-0957330. We are grateful to Bill Schwert (the editor), an anonymous referee, Snehal Banerjee, Geert Bekaert, Peter Carr, Anna Cieslak, Bjorn Eraker, Kay Giesecke, Ravi Jagannathan, Bryan Kelly (our discussant at the NBER Meeting), Robert Merton, Toby Moskowitz, Lasse Pedersen, Sergio Rebelo, Myron Scholes, Ivan Shaliastovich (our discussant in Montreal), Allan Timmermann, Jonathan Wright, Liuren Wu as well as seminar participants at Kellogg School of Management, Northwestern University, Duke University, the "Montreal 2013 Econometrics Conference: Time Series and Financial Econometrics," the 40th Annual Meeting of the Danish Econometric Society, Sandbjerg, Denmark, the European University Institute, Florence, 2013 Workshop on "Measuring and Modeling Financial Risk and High Frequency Data", the 2013 "International Conference in Financial Econometrics" at Shandong University, Jinan, China, the "40 Years after the Black-Scholes-Merton Model" conference at the Stern School of Business, October 2013, the NBER Asset Pricing Meeting at Stanford University, November 2013, Georgia Tech, Boston University, Stanford University, the AQR Insight Award, Greenwich, CT, April 2014, the 2014 Annual SoFiE Meeting, Toronto, Canada, the 2014 Australasian Econometric Society Meetings, Tasmania, Australia, the 2014 NBER Summer Institute Forecasting and Empirical Methods Meeting, and the 2014 EFA meeting, Lugano, Switzerland, for helpful comments.

*Corresponding author

Email addresses: `t-andersen@northwestern.edu` (Torben G. Andersen), `nicola.fusari@jhu.edu` (Nicola Fusari), `v-todorov@northwestern.edu` (Viktor Todorov)

1. Introduction

Equity markets are subject to pronounced time-variation in volatility as well as abrupt shifts, or jumps. Moreover, these risk features are related in intricate ways, inducing a complex equity return dynamics. Hence, the markets are incomplete and derivative securities, written
5 on the equity index, are non-redundant assets. This partially rationalizes the rapid expansion in the trading of contracts offering distinct exposures to volatility and jump risks. From an economic perspective, it suggests that derivatives data contain important information regarding the risk and risk pricing of the underlying asset. Indeed, recent evidence, exploiting parametric models, e.g., Christoffersen et al. (2012) and Santa-Clara and Yan (2010), or
10 nonparametric techniques, e.g., Bollerslev and Todorov (2011), finds the pricing of jump risk, implied by option data, to account for a significant fraction of the equity risk premium.

Standard no-arbitrage and equilibrium-based asset pricing models imply a tight relationship between the dynamics of the options and the underlying asset. This arises from the assumptions concerning the pricing of risk in the no-arbitrage setting and the endogenous
15 pricing kernels implied by the equilibrium models. A prominent example is the illustrative double-jump model of Duffie et al. (2000) in which the return volatility itself follows an affine jump diffusion. In this context, the entire option surface is governed by the evolution of market volatility, i.e., the dynamics of all options is driven by a single latent Markov (volatility) process.

Recent empirical evidence reveals, however, that the dynamics of the option surface is
20 far more complex. For example, the term structure of the volatility index, VIX, shifts over time in a manner that is incompatible with the surface being driven by a single factor, see, e.g., Johnson (2012). Likewise, Bates (2000) documents that a two-factor stochastic volatility model for the risk-neutral market dynamics provides a significant improvement
25 over a one-factor version. Moreover, Bollerslev and Todorov (2011) find that even the short-term option dynamics cannot be captured adequately by a single factor as the risk-neutral

tails display independent variation relative to market volatility, thus driving a wedge between the dynamics of the option surface and the underlying asset prices.

The objective of the current paper is to characterize the risk premia, implied by the large
30 panel of S&P 500 index options, and its relation with the aggregate market risks in the economy. As discussed in Andersen et al. (2013), the option panel contains rich information both for the evolution of volatility and jump risks and their pricing. Consequently, we let the option data speak for themselves in determining the risk premium dynamics and discriminating among alternative hypotheses regarding the source of variation in risk as well
35 as risk pricing.

The standard no-arbitrage approach starts by estimating a parametric model for the evolution of the underlying asset price. Risk premia are then introduced through a pricing kernel which implies that risk compensation is obtained through parameter shifts. This ensures, conveniently, that the risk-neutral dynamics remains within the same parametric
40 class entertained for the statistical measure. However, this approach tends to tie the equity market and option surface dynamics closely together. In particular, the equity risk premia are typically linear in volatility. In contrast, we find the options to display risk price variation that is largely unrelated to, and effectively unidentifiable from, the underlying asset prices alone.

This motivates our “reverse” approach of directly estimating a parametric model for the
45 risk-neutral dynamics exclusively from option data along with no-arbitrage restrictions based on nonparametric model-free volatility measures constructed from high-frequency data on the underlying asset. In this manner, we avoid letting a (possibly misspecified) parametric structure for the \mathbb{P} -dynamics impact the identification of option risk premia. Our goal is to
50 synthesize the option surface dynamics in a low-dimensional state vector without imposing ad hoc restrictions based on the actual return dynamics, and then proceed to explore the risk premia dynamics by combining the extracted state vector with high- and low-frequency

data on the equity index.

Following Andersen et al. (2013), we specify a general parametric model for the risk-
55 neutral return dynamics that allows for a separate left tail jump factor to impact the volatility
surface. Simultaneously, we include two distinct volatility factors and accommodate co-jumps
between returns and volatility as well as return asymmetries induced by (negative) correlation
between both diffusive and jump innovations. Moreover, we explore both Gaussian and
double-exponential specifications for the jump distributions. As such, we incorporate all
60 major features stressed in prior empirical option pricing studies and allow for various novel
features. In particular, we model the tail factor as purely jump driven, with one component
jointly governed by the volatility jumps while another is independent of spot volatility.
This feature allows the jump intensity to escalate – through so-called cross-excitation of the
jumps – in periods of crises when price and volatility jumps are prevalent, thus amplifying
65 the response of the jump intensity to major (negative) market shocks. The extended model
remains within the popular class of affine jump-diffusion models of Duffie et al. (2000) and
exemplifies the flexibility of such models for generating intricate, yet analytically tractable,
dynamic interactions between volatility and jump risks.

Of course, any tractable and parsimonious parametric model is bound to suffer from some
70 degree of misspecification. What is crucial for our analysis, however, is to avoid systematic
biases in representing the information embedded in the option panel. We do this by allowing
for a flexible state vector driving different components of the conditional risk-neutral return
distribution. Most importantly, by introducing the left tail factor, we capture systematic
variation in the corresponding part of the option surface which is missed by traditional model
75 specifications. Thus, one can view the time series realizations of our novel tail factor as a
succinct quantification of dynamic features not accommodated by existing parametric asset
pricing models.

Relative to Andersen et al. (2013), the system is generalized to allow the left tail factor

to enter directly into the spot volatility process. In addition, all three state variables may
80 impact the jump intensities. Consequently, we can explicitly test for the presence of the
tail factor in volatility, and we can gauge the significance of the different state variables in
driving separately the positive and negative jump intensities. Inference for the general model
is feasible through the approach developed in Andersen et al. (2013). However, we modify the
criterion function by including a term minimizing, not the squared, but the *relative* squared
85 option pricing error across the sample. This reduces the weight assigned to turbulent periods
where the bid-ask spreads increase sharply.

The estimation of the general system establishes that the left tail factor is an insignificant
contributor to spot volatility, even if it is correlated with the level of volatility. Moreover, it
has no presence in the right jump tail, while the left jump intensity is exclusively governed
90 by the tail factor and the more volatile and less persistent of the volatility components.
Overall, the tail factor improves the characterization of the option surface dynamics very
significantly, both in- and out-of-sample. In particular, the new model no longer systemat-
ically undervalues out-of-the-money put options following crises. Given the much improved
fit to the option surface, our extended model provides a more suitable basis for studying the
95 dynamics of the market risk premia.

Methodologically, the presence of the separately evolving tail factor implies that part
of the risk premium dynamics cannot be captured by the volatility state variables driving
the underlying asset price dynamics. This suggests that the tail factor may have predictive
power for risk premia over and above spot volatility. This is, indeed, what we find. Our tail
100 factor is important for forecasting the variance risk premium in conjunction with one of the
volatility components. In addition, the tail factor is significant in predicting excess market
returns for horizons up to one year, while the volatility factors are insignificant. These
findings rationalize why the variance risk premium is a superior return predictor relative
to volatility itself, as documented in Bollerslev et al. (2009). The key is the presence of a

105 separate factor driving the left jump tail of the risk-neutral distribution. At the same time, the tail factor provides substantially better return forecasts than the variance risk premium, or any other standard return predictor, over our sample.

110 Importantly, while the new tail factor has predictive power for risk premia, it contains no incremental information regarding the future evolution of volatility and jump risks for the underlying asset relative to the traditional volatility factors. Hence, our findings indicate that option markets embody critical information about the market risk premia and its dynamics which is essentially unidentifiable from stock market data alone. Moreover, the option surface dynamics contains information that can improve the modeling and forecasting of future volatility and jump risks, but such applications necessitate an initial untangling of the components in the risk premia that are not part of the volatility process. Overall, our 115 empirical results suggest that there is a wedge between the stochastic evolution of risks in the economy and their pricing, with the latter typically having a far more persistent response to (negative) tail events than the former.

120 Our finding of a substantial wedge between the dynamics of the option and stock markets presents a challenge for structural asset pricing models. Specifically, the standard exponentially-affine equilibrium models with a representative agent equipped with Epstein-Zin preferences imply that the ratio of the risk-neutral and statistical jump tails is constant. On the contrary, the new factor, extracted from the option data, drives the risk-neutral left jump tail but has no discernable impact on the statistical jump tail. We conjecture that this wider gap between fundamentals and asset prices may be accounted for through an extension 125 of the preferences via some form for time-varying risk aversion and/or ambiguity aversion towards extreme downside risk.

The rest of the paper is organized as follows. Section 2 describes the data. Section 3 presents our three-factor model which, apart from the modeling of the jump distributions, 130 encompasses most existing models in the empirical literature. Section 4 introduces the es-

estimation methodology and discusses the parameter estimates. Section 5 explores model fit and presents different robustness checks. This analysis brings out some of the mechanisms behind the improved fit of our model. Section 6 is dedicated to an out-of-sample analysis. In Section 7 we exploit the estimation results to study the risk premium dynamics and its implication for return and variance predictability. Our findings are contrasted to corresponding predictability results implied by popular structural equilibrium models. Section 8 concludes. Details on various aspects of the analysis are collected in an Appendix. A number of additional robustness checks and further details on the estimation are provided in a Supplementary Appendix.

2. Data and Preliminary Analysis

We use European style S&P 500 equity-index (SPX) options traded at the CBOE. We exploit the closing bid and ask prices reported by OptionMetrics, applying standard filters and discarding all in-the-money options, options with time-to-maturity of less than 7 days, as well as options with zero bid prices. For all remaining options, we compute the mid bid-ask Black-Scholes implied volatility (IV). The data spans January 1, 1996–April 23, 2013. It is further divided into an in-sample period covering January 1, 1996–July 21, 2010, and an out-of-sample period consisting of July 22, 2010–April 23, 2013. Following earlier empirical work, e.g., Bates (2000) and Christoffersen et al. (2009), we sample every Wednesday.¹ The in-sample period includes 760 trading days, and the estimation is based on an average of 234 bid-ask quotes per day. The out-of-sample period contains 142 trading days and features a much higher number of active quotes at any point in time, so we exploit an average of 708 option contracts daily from this sample. The nonparametric estimate of volatility used for penalizing the objective function below is constructed from one-minute data on the S&P

¹Due to extreme violations of no-arbitrage-conditions, we replaced October 8, 2008, with October 6, 2008.

500 futures covering the time span of the options. The same data are used to construct
 155 measures of volatility and jump risks for the predictive regressions in Section 7. Finally, we
 employ the returns on the SPY ETF traded on the NYSE, which tracks the S&P 500 index
 portfolio, and the 3-month T-bill rate to proxy for the risk-free rate, when implementing
 these regressions.

2.1. The Option Panel

160 We denote European-style out-of-the-money (OTM) option prices for the asset X at time
 t by $O_{t,k,\tau}$. Assuming frictionless trading in the options market and denoting with \mathbb{Q} the
 risk-neutral measure, the option prices at time t are given as,

$$O_{t,k,\tau} = \begin{cases} \mathbb{E}_t^{\mathbb{Q}} \left[e^{-\int_t^{t+\tau} r_s ds} (X_{t+\tau} - K)^+ \right], & \text{if } K > F_{t,t+\tau} , \\ \mathbb{E}_t^{\mathbb{Q}} \left[e^{-\int_t^{t+\tau} r_s ds} (K - X_{t+\tau})^+ \right], & \text{if } K \leq F_{t,t+\tau} , \end{cases} \quad (1)$$

where τ is the tenor of the option, K is the strike price, $F_{t,t+\tau}$ is the futures price for
 the underlying asset at time t referring to date $t + \tau$, for $\tau > 0$, $k = \ln(K/F_{t,t+\tau})$ is the
 165 log-moneyness, and r_t is the instantaneous risk-free interest rate. Finally, we denote the
 annualized Black-Scholes implied volatility corresponding to the option price $O_{t,k,\tau}$ by $\kappa_{t,k,\tau}$.
 This merely represents an alternative notational convention, as the Black-Scholes implied
 volatility is a strictly monotone transformation of the ratio $\frac{e^{r_{t,t+\tau}} O_{t,k,\tau}}{F_{t,t+\tau}}$, where $r_{t,t+\tau}$ denotes
 the risk-free rate over the period $[t, t + \tau]$.

170 The empirical work explicitly accounts for measurement error in the option prices. We
 denote the average of the bid and ask quotes (expressed in Black-Scholes implied volatility
 units) by $\bar{\kappa}_{t,k,\tau}$, and view this as a noisy observation of underlying value. To the extent
 the measurement errors are not strongly correlated across a large fraction of the surface,
 we improve the efficiency of the inference by incorporating the full option cross-section in
 175 our estimation and testing procedures, effectively averaging out idiosyncratic observation

errors. The size of the spread varies over time and is positively correlated with the volatility level. In addition, there are systematic differences in the relative spread across moneyness. For example, the spread is about 8% of the mid-quote for deep OTM puts, on average, implying that a typical implied volatility reading of 40% is associated with bid and ask quotes of 38.4% and 41.6%. Similarly, for an IV of 18% for at-the-money (ATM) options, the quotes are generally around 17.6%-18.4%, while a typical set of quotes for far OTM calls are 18.8%-21.2% for a mid-point value of 20%.

The options underlying the IV surface are highly heterogeneous in terms of moneyness and tenor across time. To facilitate comparison, we create a uniform set of regions based on the option characteristics. Specifically, we define the *volatility-adjusted moneyness*, m , at time t for tenor τ , by standardizing the log-moneyness with the ATM IV,

$$m = \frac{\ln(K/F_{t,t+\tau})}{\kappa_{t,0,\tau} \cdot \sqrt{\tau}}. \quad (2)$$

Table 1 shows how the observations in our sample are distributed across the option surface. The four regions of moneyness represent deep OTM put options, OTM put options, ATM options and OTM call options, while the two categories for time-to-maturity provide a rough split into short versus long dated options. Not surprisingly, there is particularly good coverage for ATM options, which represent over 44% of the in-sample observations. The quotes for the OTM call options are somewhat limited and amount to almost 16% of the total options quotes, roughly matching the proportion of deep OTM put options.

In the out-of-sample period, the daily number of active quotes is much higher, especially for deep OTM options. Since we would like to compare model performance across the two samples, we have truncated the set of OTM options included in the recent period to lie within the boundaries of -7.1 for the puts and 2.4 for the calls. These cut-offs correspond to the average minimum and maximum moneyness of the option quotes for our in-sample period.

	1996:1-2010:7		2010:7-2013:4	
	$\tau \leq 60$	$\tau > 60$	$\tau \leq 60$	$\tau > 60$
$m \leq -3$	10.36	5.23	18.46	8.62
$-3 < m \leq -1$	12.34	11.89	12.31	11.03
$-1 < m \leq 1$	19.58	24.77	14.58	17.90
$m > 1$	8.71	7.13	10.34	6.76
All	50.98	49.02	55.69	44.31

Table 1: **Relative Number of Contracts.** We report the percentage of option contracts that, on average, fall within the different combinations of moneyness and tenor for the indicated sample.

This standardization limits the heterogeneity across the samples. The relative proportion of
200 OTM calls and puts is stable, but we observe a non-trivial shift from ATM to deep OTM
put options, with the former now representing about 32.5% and the latter 27% of the overall
observations. To the extent variation in the pricing of deep OTM put option prices is harder
to accommodate than for ATM prices, this composition effect will – all else equal – imply a
worse out-of-sample fit than would otherwise be observed.

205 2.2. The Option Surface Characteristics

The option IV surface displays a highly persistent and nonlinear dynamics which is
difficult to convey effectively through a few summary measures. We provide a couple of
alternative depictions that highlight different aspects of the dynamics. The first approach
emphasizes the evolution of separate *option surface characteristics*, as defined below. The
210 second approach consists of a standard principal components analysis of the IV surface.

The option characteristics are plotted on Figure 1. The *level* captures the average IV for
ATM short-dated options, the *term structure* reflects the difference between the IV of long
and short maturity ATM options, the *skew* measures the IV gap between short-dated OTM
put and OTM call options, and, finally, the *skew term structure* is the difference between
215 the skew computed from long- and short-dated options. The exact definitions are provided
in the caption to Figure 1. Note, in particular, that we define the short- and long-term skew

symmetrically with respect to the degree of volatility-adjusted moneyness for the left and right tail, as advocated by Bates (1991).

The IV level displays occasional erratic spikes to the upside, but also displays strong persistence, as expected for a series reflecting the general level of volatility. Inspecting the remaining three panels, we notice a considerable degree of commonality. Every major spike in the IV level is visible in the other characteristics.

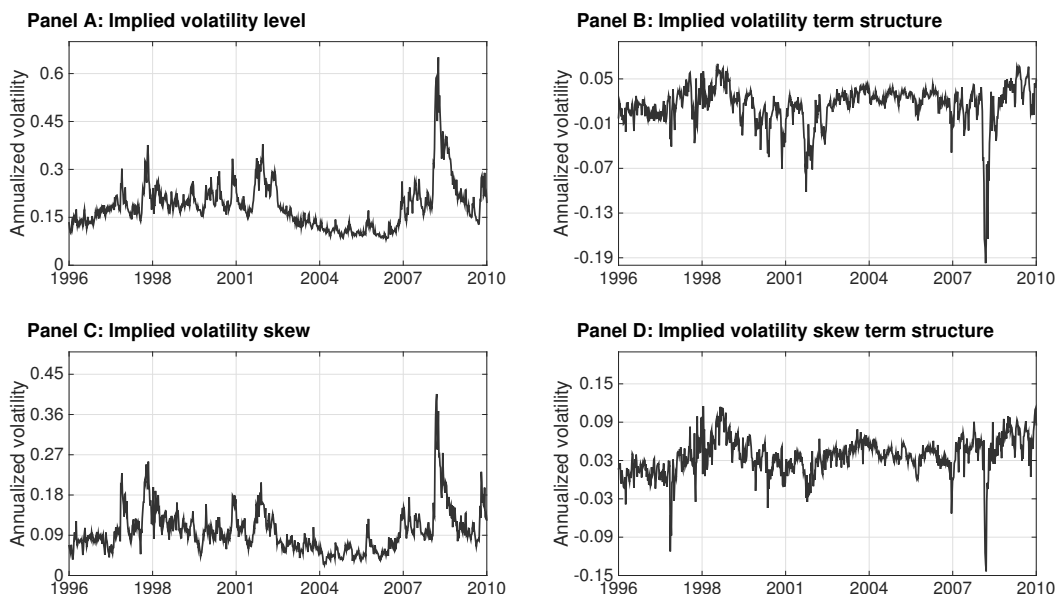


Figure 1: **Implied Volatility (IV) Surface Characteristics**. Top left Panel: The IV Level is the average IV for short ATM options. Top Right Panel: The IV Term Structure is the difference in IV between long- and short-dated ATM options. Bottom left Panel: The IV Skew is the difference between the IV of short-dated OTM put and OTM call options. Bottom right Panel: The Skew Term Structure is the difference between the long- and short-dated skew, with the long skew defined analogously to the short skew. Short-dated options are those with 0.1 years to maturity and long-dated options have 0.8 year to maturity. ATM options have volatility-adjusted moneyness m equal to zero; OTM put options have $m = -2$; OTM call options have $m = 2$.

Table 2 supplements Figure 1 with summary statistics for the IV surface characteristics. The correlation matrix confirms the strong covariation between the IV level and the remaining features. Moving to the other characteristics, we see that the IV term structure

is moderately positive, apart from episodic large negative outliers. The skew is consistently positive, exceeding 5% over the vast majority of the sample and averaging 10%. The skew also displays pronounced persistence and is particularly elevated when markets are turbulent. Finally, the skew term structure is mostly positive, but spikes downward during steep market declines, indicating a dramatic flattening of the “smirk” at the onset of market crises. This feature accounts for a great deal of variation in the surface, as the skew is negatively correlated with the skew term structure. Specifically, when the skew steepens drastically, the effect is much less pronounced at longer maturities. Hence, this type of excitement of the short left part of the IV surface must be associated with shocks to volatility and jump intensities of moderate persistence.

While there is a clear dependence between the option characteristics, both Figure 1 and Table 2 suggest that the dynamics of the IV level cannot account for the overall surface dynamics. For example, the 1997 and 1998 crises have a much more pronounced and persistent effect on the skew than the IV level. Likewise, the aftermath of the 1998 Russian crisis is associated with a historically high upward-sloping term structure, while the IV level is close to its historical mean. In contrast, other periods with similar IV levels feature much flatter IV term structures. Hence, we need a multi-factor model to capture the dynamic dependencies between the option surface characteristics, as also concluded in Christoffersen et al. (2009).

	Summary statistics			Correlation Matrix			
	Mean	Median	Std	Level	TS	Skew	Skew TS
Level	0.19	0.18	0.08	1.00	-0.69	0.89	-0.24
TS	0.01	0.02	0.03	-	1.00	-0.57	0.69
Skew	0.10	0.09	0.05	-	-	1.00	-0.31
Skew TS	0.04	0.04	0.03	-	-	-	1.00

Table 2: **Summary Statistics and Correlation Matrix for Option Characteristics.** The statistics for the implied volatility Level, Term Structure (TS), Skew, and Skew Term Structure are computed over the in-sample period, January 1996–July 2010.

Turning to the principal component (PC) analysis, Figure 2 depicts the in-sample realizations of the first four PCs of the IV surface. It is evident that the first PC is closely related to the IV level, while the second PC displays commonality with the IV term structure. However, the last two PCs appear largely unrelated to the characteristics depicted in Figure 1. The first PC captures about 96.4% of the total variation, while the following PCs account for, respectively, 2.1%, 0.7% and 0.3%. Clearly, there is a dominant level type effect, but this “factor” also accounts for a great deal of variation in the skew, term structure and skew term structure, leaving, relatively speaking, only minor residual variation to explain for the remaining PCs.

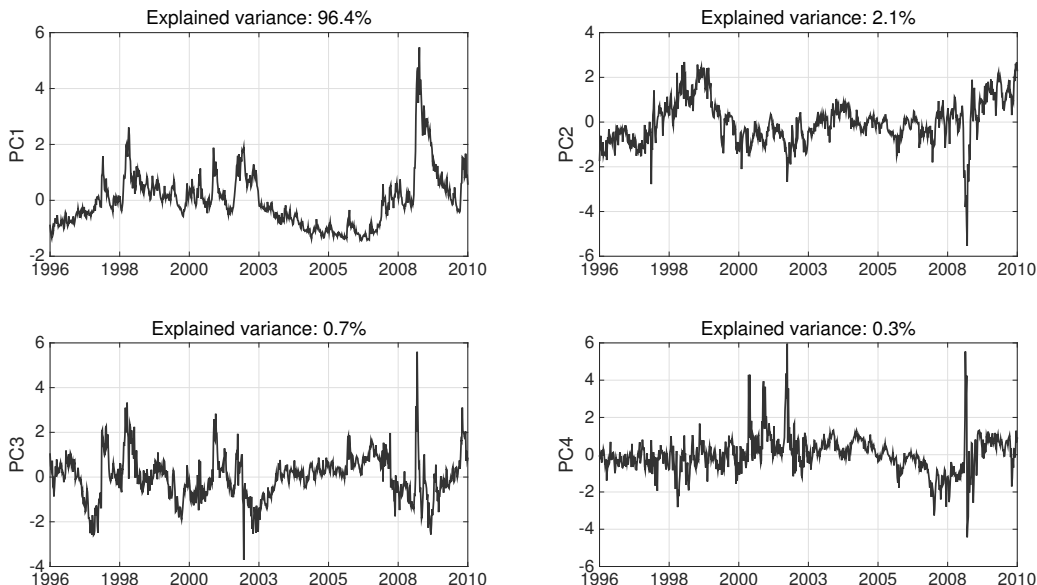


Figure 2: **Principal Components of the Implied Volatility Surface.** The panels depict the first four principal components extracted from the S&P 500 IV surface from January 1996 to July 2010. On each day we interpolate the IV surface to generate standardized options with the same volatility-adjusted moneyness, m , and tenor across the sample. Specifically, we obtain option prices for m in the set $\{-4, -3, -2, -1, -0, 1, 2\}$ and tenor equal to three values, $\{0.1, 0.3, 0.8\}$ (in years). This produces a total of 21 synthesized option contracts per day. For each panel, we also report the percentage of the overall variation explained by the given principal component.

To further explore how the PCs interact with the IV surface characteristics, Table 3

255 reports on the in-sample regression of characteristics on PCs. The table confirms the strong
association of the first PC with the IV level, featuring a t -statistic beyond 300. For this PC,
we also obtain the negative association with the IV and skew term structures and positive
relation with the skew, matching the correlation patterns for the IV level in Table 2. In
addition, we find the second PC to be associated with the IV term structure, corroborating
260 the visual impression from Figure 2. The third PC is associated with the skew as well as
the skew term structure and level. However, the skew is much more strongly associated
with the first PC so, effectively, the third PC captures only residual skew variation that is
largely orthogonal to the level. Finally, the fourth PC has no clear association with any
of the characteristics. In particular, the variation in the skew term structure is effectively
265 accounted for through the first two or three PCs.

	Level	TS	Skew	Skew TS
PC1	0.19 (343.79)	-0.04 (-60.84)	0.11 (133.05)	-0.01 (-6.42)
PC2	-0.24 (-63.65)	0.40 (87.14)	-0.05 (-9.19)	0.41 (41.04)
PC3	-0.14 (-21.49)	-0.08 (-10.48)	0.45 (43.81)	-0.21 (-11.82)
PC4	-0.05 (-5.07)	-0.08 (-6.88)	-0.36 (-23.36)	0.03 (1.06)
R2	0.99	0.94	0.96	0.71
AC(1)	0.66	0.60	0.32	0.44
AC(2:10)	0.39	0.26	0.21	0.26
AC(11:20)	0.27	0.16	0.12	0.16

Table 3: **Relating Option Characteristics and Principal Components.** We report the coefficients with t -statistics (in parentheses) and the R^2 from the linear regression of different options characteristics (level, term structure, slope, and slope term structure) on the first four principal components extracted from the S&P 500 implied volatility surface from January 1996 to July 2010. We also report the first sample autocorrelation coefficient and the average sample autocorrelation coefficient over two-to-ten and eleven-to-twenty lags of the regression residuals.

These observations have a number of implications. First, there is no simple mapping between PCs and characteristics. The latter are intrinsically interconnected and covary strongly, so factors associated with the PCs will generally exert a significant joint impact on multiple characteristics. Second, the difficulty of separating the forces driving the individual

270 characteristics is, of course, a general feature of systems with pronounced nonlinearities. We see further evidence of potential nonlinearity in the strong serial correlation in the residuals of the regressions in Table 3. The first order autocorrelation coefficient is very large across all the characteristics and die out extremely slowly, suggesting highly persistent deviations from the linear approximation associated with the regression analysis. Third, the persistent
275 residuals may be due to missing factors and, indeed, we find standard tests for the number of factors, see, e.g., Bai and Ng (2002), to indicate 7 to 8 factors. However, given the nonlinear association between option IV and (latent) factors, this likely reflects the failure of the linear approximation rather than the true number of underlying (linear) factors.²

In summary, accounting for a given model’s ability to track the IV surface dynamics
280 provides an intuitive way to highlight the implications of model misspecification. Indeed, we later illustrate the quality of fit by comparing the model-implied and observed IV surface characteristics. On the other hand, there is no direct association between the inability to fit the dynamics of a specific set of characteristics and the lack of a given factor, because the factors’ impact on the option IVs are highly nonlinear and create correlated dynamic
285 interactions across the characteristics.

3. Parametric Modeling of the Option Panel

We turn next to parametric modeling of the options with the goal of succinctly capturing the IV surface dynamics via a low-dimensional state vector. We adopt a general-to-specific approach. The proposed model subsequently serves as the basis for our analysis of the equity
290 and variance risk premia. The initial decision concerns the number of latent state variables

²For a simple illustration, we calibrated a one-factor Heston model and derived the sensitivity of the IV surface to the volatility factor. For a given location in the surface, i.e., a given mildly OTM option, the sensitivity (derivative of the option IV with respect to volatility) will typically vary dramatically with the level of volatility. Thus, strongly correlated approximation errors will arise from linearizing the dependence of the surface characteristics to factors, as the true sensitivities fluctuate strongly over time. This illustration is provided in our Supplementary Appendix.

to include. The vast majority of empirical option pricing studies employs a single stochastic volatility factor, but the literature on estimating the return dynamics under the physical measure as well as a few option pricing studies, e.g., Bates (2000), Christoffersen et al. (2009), Christoffersen et al. (2012), and Andersen et al. (2013), point to a minimum of two factors.

295 This is also consistent with our descriptive analysis of the IV surface in Section 2. Hence, we follow Andersen et al. (2013) in proposing a general three-factor model which, apart from the specification of the jump distribution, embeds most existing continuous-time models in the literature as special cases. We document below that exponentially distributed price jumps provide a superior fit relative to the more commonly adopted Gaussian specification, 300 justifying the alternative representation in our benchmark model.

Our three-factor model for the risk-neutral equity index dynamics is given by the following extension of the representation in Andersen et al. (2013),

$$\begin{aligned}
\frac{dX_t}{X_{t-}} &= (r_t - \delta_t) dt + \sqrt{V_{1,t}} dW_{1,t}^{\mathbb{Q}} + \sqrt{V_{2,t}} dW_{2,t}^{\mathbb{Q}} + \eta \sqrt{U_t} dW_{3,t}^{\mathbb{Q}} + \int_{\mathbb{R}^2} (e^x - 1) \tilde{\mu}^{\mathbb{Q}}(dt, dx, dy), \\
dV_{1,t} &= \kappa_1 (\bar{v}_1 - V_{1,t}) dt + \sigma_1 \sqrt{V_{1,t}} dB_{1,t}^{\mathbb{Q}} + \mu_1 \int_{\mathbb{R}^2} x^2 1_{\{x < 0\}} \mu(dt, dx, dy), \\
dV_{2,t} &= \kappa_2 (\bar{v}_2 - V_{2,t}) dt + \sigma_2 \sqrt{V_{2,t}} dB_{2,t}^{\mathbb{Q}}, \\
dU_t &= -\kappa_u U_t dt + \mu_u \int_{\mathbb{R}^2} [(1 - \rho_u) x^2 1_{\{x < 0\}} + \rho_u y^2] \mu(dt, dx, dy),
\end{aligned} \tag{3}$$

305 where $(W_{1,t}^{\mathbb{Q}}, W_{2,t}^{\mathbb{Q}}, W_{3,t}^{\mathbb{Q}}, B_{1,t}^{\mathbb{Q}}, B_{2,t}^{\mathbb{Q}})$ is a five-dimensional Brownian motion with $\text{corr}(W_{1,t}^{\mathbb{Q}}, B_{1,t}^{\mathbb{Q}}) = \rho_1$ and $\text{corr}(W_{2,t}^{\mathbb{Q}}, B_{2,t}^{\mathbb{Q}}) = \rho_2$, while the remaining Brownian motions are mutually independent. In addition, μ is an integer-valued measure counting the jumps in the price, X , as well as the state vector, (V_1, V_2, U) . The corresponding (instantaneous) jump intensity, under the risk-neutral measure, is $dt \otimes \nu_t^{\mathbb{Q}}(dx, dy)$. The difference $\tilde{\mu}^{\mathbb{Q}}(dt, dx, dy) =$ 310 $\mu(dt, dx, dy) - dt \nu_t^{\mathbb{Q}}(dx, dy)$, constitutes the associated martingale jump measure.

The jump specification involves two separate components, x and y . The former captures co-jumps that occur simultaneously in the price, the first volatility factor, V_1 , and, potentially, in the U factor (if $\rho_u < 1$), while the y jumps represent independent shocks to the U factor.³ The compensator characterizes the conditional jump distribution and is given by,

$$\frac{\nu_t^{\mathbb{Q}}(dx, dy)}{dxdy} = \begin{cases} (c^-(t) \cdot 1_{\{x < 0\}} \lambda_- e^{-\lambda_- |x|} + c^+(t) \cdot 1_{\{x > 0\}} \lambda_+ e^{-\lambda_+ x}), & \text{if } y = 0, \\ c^-(t) \lambda_- e^{-\lambda_- |y|}, & \text{if } x = 0 \text{ and } y < 0. \end{cases} \quad (4)$$

315

The first term on the right hand side, referring to the $x \neq 0, y = 0$ case, reflects co-jumps in price and volatility, while the second term, $x = 0, y < 0$, captures independent shocks to the U factor. Hence, the individual (strictly positive) jumps in U are either independent from V_1 or proportional to the (simultaneous) jump in V_1 . Following Kou (2002), we model the price jumps as exponentially distributed, with separate tail decay parameters, λ_- and λ_+ , for negative and positive jumps. Moreover, for parsimony, the independent shocks to the U factor is distributed identically to the negative price jumps. Finally, the time-varying jump intensities are governed by the $c^-(t)$ and $c^+(t)$ coefficients. These coefficients evolve as affine functions of the state vector,

325

$$c^-(t) = c_0^- + c_1^- V_{1,t-} + c_2^- V_{2,t-} + U_{t-}, \quad c^+(t) = c_0^+ + c_1^+ V_{1,t-} + c_2^+ V_{2,t-} + c_u^+ U_{t-}. \quad (5)$$

This representation involves a large set of parameters that can be hard to identify separately. At the estimation stage, we eliminate those that are insignificant and have no discernible impact on model fit. However, generality along this dimension is important, as the jump specification turns out to be critical for a suitable representation of the IV surface

330

³The latter can also generate a jump in return volatility if $\eta > 0$.

dynamics. We note that for identification purposes, we set the coefficient in front of U in $c^-(t)$ to unity, and hence the value of U directly signifies its contribution to the negative jump intensity.⁴

335 Our three-factor model possesses a number of distinctive features. The factors (V_1, V_2, U) drive both the diffusive volatility and the jump intensities. V_1 and V_2 are always present in the diffusive volatility, as in traditional multi-factor volatility models, while U contributes to diffusive volatility only if $\eta > 0$. In fact, the constrained model arising for $\eta = 0$ is of separate interest. It implies that the factor U affects only the jump intensities, with no impact on
340 diffusive volatility. Furthermore, in an extension to existing option pricing models, we allow positive and negative jump intensities to have different loadings on the latent factors. In particular, some factors affect only positive or only negative jump intensities. Such flexibility in modeling the jump intensities is important given the nonparametric evidence in Bollerslev and Todorov (2011).

345 The jump modeling also involves several novel features. First, the price jumps are exponentially distributed. This is unlike most earlier studies which rely on Gaussian price jumps, following Merton (1976).⁵ Next, the jumps in the factor V_1 are linked deterministically to the price jumps, with squared price jumps impacting the volatility dynamics in a manner reminiscent of discrete GARCH models.⁶ For parsimony and ease of identification, we allow

⁴The formal inference in Andersen et al. (2013) provides strong evidence for the presence of a separately evolving left jump tail factor like U in the risk-neutral return dynamics, while it is unclear if U also directly impacts spot volatility. As such, we let U enter the left jump intensity with a unitary coefficient. This resolves identification issues that arise regarding the scale of U versus the loading coefficient for U in the jump intensity. It is analogous to the imposition of a unitary coefficient for the volatility components in the return dynamics in equation (3).

⁵Bates (2012) studies the option pricing implications of models with exponential and Gaussian jumps. He finds them to be broadly similar for short-maturity options that are not deep OTM.

⁶Our modeling of the volatility jumps, and their dependence with the price jumps, deviates from earlier empirical option pricing studies, e.g., Duffie et al. (2000), who model volatility jumps as exponentially distributed. In our case, they are the squares of exponentially distributed random variables, and hence much fatter tailed. This enhances the reaction of volatility to large price shocks. Finally, our modeling implies a nonlinear deterministic link between price and volatility jumps, unlike Duffie et al. (2000). Of course, there is overwhelming empirical support for GARCH like dynamics in volatility, similar to the continuous time

350 only the negative price jumps to impact the volatility dynamics. Finally, U is driven in part
 by the squared negative price jumps and in part by independent jumps, with the parameter
 ρ_u controlling the contribution of each component in the dynamics of U . As such, the model
 accommodates both perfect dependence ($\rho_u = 0$) and full independence ($\rho_u = 1$) between
 the jump risks of V_1 and U . Moreover, these state variables, governing critical features of
 355 the option surface dynamics, are related through the time-variation in the jump intensity.
 Our specification allows for “cross-excitation” in which jumps in V_1 enhance the probability
 of future jumps in U , and vice versa.⁷

Differences in the jump distributions aside, our model nests most existing models. For
 the one-factor setting, with V_2 and U absent, we recover the double-jump volatility model
 360 of Duffie et al. (2000), estimated using options data by Broadie et al. (2007). In the two-
 factor setting, with U absent and excluding volatility jumps, we obtain the Bates (2000)
 jump-diffusion, and further ruling out price jumps leads to the two-factor diffusive model
 of Christoffersen et al. (2009). The key difference in our model from existing work is the
 separation of the left jump intensity from the volatility (and its components) and the right
 365 jump intensity (through the U factor).

We know of only two prior instances where this type of separation is contemplated.
 Santa-Clara and Yan (2010) model jump intensity by a separate diffusive factor that can be
 correlated with volatility, which itself follows a diffusion. Hence, the model does not include
 volatility jumps, critical for fitting the option surface, as noted by Broadie et al. (2007) and
 370 further confirmed here. Christoffersen et al. (2012) consider a discrete-time GARCH model

specification adopted here.

⁷We stress that the model (3) still belongs to the affine family covered by Duffie et al. (2003) and, as
 shown in Andersen et al. (2013), the following parameter constraints ensure covariance stationarity of the
 latent factors,

$$\kappa_1 > \frac{2c_1^- \mu_1}{\lambda_-^2}, \quad \text{and} \quad \kappa_u > \frac{2\kappa_1 \mu_u}{\kappa_1 \lambda_-^2 - 2c_1^- \mu_1}, \quad \text{and} \quad \kappa_2 < 0, \quad \text{and} \quad \sigma_i^2 \leq 2\kappa_i \bar{v}_i, \quad i = 1, 2.$$

with conditionally Gaussian and non-Gaussian innovations (“jumps” of Merton type) where conditional volatility and jump intensity are driven by past squared innovations. This model does not allow for closed-form solutions for the option prices, complicating inference from the option surface. Our model differs from these two papers along several dimensions crucial for the analysis of risk premia. First, we only model the risk-neutral distribution and do not
 375 assume any structure under \mathbb{P} . Thus, we do not import information from the physical return dynamics (other than no-arbitrage restrictions). This is critical for our subsequent findings regarding the drivers of risks and risk premia in Section 7. Second, we separate the dynamics of the left and right jump intensities which is important for the pricing of short maturity OTM
 380 puts and calls. Third, we adopt the double-exponential return jump distribution, providing a superior fit to the short maturity OTM options. Fourth, our specification involves cross-excitation in the jump and volatility dynamics, leading to improved characterization of longer maturity options, particularly in the aftermath of volatile episodes in the sample.

In summary, the main departure from prior work stems from the inclusion of the new U
 385 factor. Given the rather unconventional representation, we briefly discuss how this factor enhances the features of the risk-neutral dynamics. It is best seen by focusing on a restricted model where we eliminate U from the diffusive volatility, i.e., set $\eta = 0$, and further let $\rho_u = 0$, so that there is no independent jump component driving U . In this scenario, there is no distinct source of risk impacting U – it is driven solely by the squared negative price
 390 jumps. Nonetheless, U affects the jump intensities, and hence the option surface, separately from V_1 . That is, to convey the current state of the system, U must be included among the components of the state vector.⁸ In other words, even if the source of risk in U is spanned

⁸This is a reflection of the fact that there is no direct association between the dimensionality of the sources of risk and the dimension of the state vector required to characterize the conditional dynamics of the system. This phenomenon arises naturally in continuous-time ARMA models, see, e.g., Brockwell (2001). It is also a well-known feature of the so-called quadratic term structure models, see, e.g. Ahn et al. (2002) and Leippold and Wu (2002).

by the jumps in X and V_1 , U is still necessary for characterizing the conditional *risk-neutral* distribution of future log returns or predicting the future evolution of the factors, even after
 395 controlling for the current values of V_1 and V_2 . Of course, the role of U only expands, if it is subject to independent shocks as well. In the empirical section below, we detail how the U factor impacts the IV surface characteristics over time.

The model in equation (3) pertains to the risk-neutral dynamics of X . However, due to the equivalence of \mathbb{Q} and \mathbb{P} , the assumed dynamics have implications for the dynamics of
 400 X under \mathbb{P} as well. In general, these implications are limited to those features of model (3) which hold almost surely. They consist of the following. First, the spot diffusive variance is invariant to the change of measure. In the model, this is given by

$$V_t = V_{1,t} + V_{2,t} + \eta^2 U_t. \quad (6)$$

Second, regarding the jumps, the only property that applies almost surely is the identity of the realized jumps in the returns and state variables. In particular,

$$\Delta V_{1,t} = \mu_1 (\Delta \log(X))^2 1_{\{\Delta \log(X) < 0\}}, \quad (7)$$

405 and, if $\rho_u = 0$, we also have,

$$\Delta U_t = (\Delta \log(X))^2 1_{\{\Delta \log(X) < 0\}}, \quad (8)$$

under both measures.

In most empirical option pricing applications, additional assumptions are invoked when changing measure from \mathbb{P} to \mathbb{Q} . For example, it is commonly assumed that the model class is identical, and affine, under both measures. This is convenient as affine models offer a
 410 great deal of tractability. However, this approach severely restricts the dynamics of the risk

premiums. In addition, such “structure preserving transformations” (SPTs) impose auxiliary restrictions, extending to the model parameters. In particular, in our affine setting, the SPT assumption implies that $\sigma_1, \sigma_2, \eta, \rho_1, \rho_2, \rho_u, \mu_1$ and κ_3 are identical under \mathbb{P} and \mathbb{Q} , while the remaining parameters may differ.

415 Given the above discussion, it is clear that data on the underlying equity-index values can be helpful in the estimation of the risk-neutral model. Below, we impose the pathwise (almost sure) restriction regarding the spot variance in estimation. Given the difficulty in recovering spot volatility jumps from high-frequency data – due both to estimation uncertainty and lack of overnight observations – we do not impose restrictions regarding the pathwise (realized) price and volatility jump relationship implied by our risk-neutral model. Finally, if one 420 constrains the pricing of risk through a SPT from \mathbb{P} to \mathbb{Q} , additional information from the \mathbb{P} dynamics can be “imported” from the underlying return data during estimation of the risk-neutral dynamics. This comes, however, with the risk of severe model misspecification. As we document below, the option panel is very informative about the risk-neutral dynamics, 425 so we avoid auxiliary restrictions that may induce model misspecification with unpredictable impact on our inference for the risk premia.

4. Estimation

4.1. Estimation Approach

The development of formal tools for parametric inference in the context of an option 430 panel is challenging. There are pronounced time series dependencies in the latent volatility components and, potentially, the jump intensities. At the same time, sizeable bid-ask spreads influence the observed prices and quotes for the options. These measurement errors are strongly heterogeneous and correlated with the overall return variation. Finally, there are no-arbitrage constraints that, one, at any point in time link the individual option 435 prices across strikes, and, two, equate the spot diffusive volatility for the underlying asset

(imperfectly observable from high-frequency returns) with the volatility implied by the contemporaneous state vector (also extracted with a degree of statistical error) for every option cross-section. Consequently, we adapt the parametric estimation and inference approach put forth in Andersen et al. (2013) that is designed to deal with this type of environment. It
440 exploits in-fill asymptotics in the option cross-section, i.e., it operates under the assumption that, for a small set of maturities which may vary from day to day, option prices are observed across a broad range of strikes with only small gaps between the exercise prices.

The approach provides consistent period-by-period estimates for the state vector along with valid asymptotic inference for the state vector and model parameters as well as the fit to
445 specific regions of the IV surface on any given day. This is possible due only to the adoption of the in-fill asymptotic scheme for the option cross-section.⁹ In practice, this reflects the actual structure of our panel. The option quotes are clustered closely in the strike range, while we use only weekly observations of the option cross-section. Thus, the well-recognized advantages of inference via “high-frequency” data apply naturally to the cross-section, not
450 the time series, in our setting.

The wealth of information embedded in the option cross-section is, of course, well-recognized. It is known to facilitate nonparametric extraction of the conditional risk-neutral density for the underlying asset returns across the maturities available on a given day. Through the imposition of a general parametric structure and inference procedure, we let the
455 dynamic evolution of the conditional densities speak to the number of factors as well as the intertemporal variation in volatility and jump intensities. Given the identified factors and model parameters, the individual cross-section identifies the current state vector. In fact, theoretically, the entire system can be identified and estimated consistently from a single

⁹Alternative inference techniques can potentially generate unbiased estimates for the state vector realizations, determining the values of the volatility components and jump intensities, but cannot achieve consistency, thus rendering formal inference regarding the state vector and IV surface fit on a period-by-period basis infeasible.

cross-section. However, the identification from a single option surface is weak. The use of a
 460 large number of surfaces, i.e., an option panel, allows the variation in the state vector over
 time to assist in identifying the underlying structure governing the option prices and also
 helps diversify the idiosyncratic measurement errors.¹⁰

We denote the parameter vector of model (3) by θ and the state vector at time t by
 $\mathbf{Z}_t = (V_{1,t} \ V_{2,t} \ U_t)$. Further, the model-implied Black-Scholes IV is given by $\kappa(k, \tau, \mathbf{Z}_t, \theta)$
 465 and the model-implied diffusive spot variance by $V(\mathbf{Z}_t, \theta) = V_{1,t} + V_{2,t} + \eta^2 U_t$. Letting n
 denote the (equidistant) frequency by which we sample the high-frequency asset returns, our
 estimator takes the form,

$$\left(\{\widehat{V}_{1,t}^n, \widehat{V}_{2,t}^n, \widehat{U}_t^n\}_{t=1,\dots,T}, \widehat{\theta}^n \right) = \underset{\{\mathbf{Z}_t\}_{t=1,\dots,T}, \theta \in \Theta}{\operatorname{argmin}} \sum_{t=1}^T \left\{ \frac{\text{Option Fit}_t + \lambda \times \text{Vol Fit}_t}{V_t^{ATM}} \right\}, \quad (9)$$

$$\text{Option Fit}_t = \frac{1}{N_t} \sum_{j=1}^{N_t} (\bar{\kappa}_{t,k_j,\tau_j} - \kappa(k_j, \tau_j, \mathbf{Z}_t, \theta))^2, \quad \text{Vol Fit}_t = \left(\sqrt{\widehat{V}_t^{(n,m_n)}} - \sqrt{V(\mathbf{Z}_t, \theta)} \right)^2,$$

where $\widehat{V}_t^{(n,m_n)}$ is a nonparametric estimator of the diffusive spot variance constructed from
 470 the underlying intraday asset prices, as detailed in the Appendix, and V_t^{ATM} is the squared
 short term ATM Black-Scholes IV.¹¹ Finally, λ is a tuning parameter which we set to 0.2.¹²

The estimator (9) minimizes the weighted mean squared error in fitting the panel of

¹⁰On the other hand, one year of option data – along with the high-frequency returns used to enforce the (statistical) equality of spot volatility across the \mathbb{P} to \mathbb{Q} measures – usually suffices for reasonable identification.

¹¹This measure is obtained for the shortest available maturity on day t and for the option closest to at-the-money, with the associated forward rate deduced from put-call parity.

¹²In general, given the noise in the high-frequency spot volatility estimate, we should pick a relatively low value for λ . In the Supplementary Appendix, we report further evidence corresponding to different values of λ .

observed option IVs, with a penalization term that reflects the deviation of the model-
implied spot variance from a model-free spot variance estimate. The presence of the volatility
475 fit in the objective function not only facilitates the incorporation (statistically) of the no-
arbitrage constraint, but also serves as a regularization device for the estimation by penalizing
parameter values that imply “unreasonable” volatility levels. Moreover, the standardization
by V_t^{ATM} implies we weigh observations on high and low volatility days differently. This
improves efficiency as the measurement errors in the option prices and the estimation errors
480 for the state vector generally rise with market volatility.¹³

The estimator (9) is derived via joint optimization over parameters and state vector
realizations. This high-dimensional problem is tractable due to the particular form of our
objective function: the terms corresponding to a given observation time depend on the state
vector only through the option prices and nonparametric spot volatility estimate for that
485 particular day. Thus, given a candidate θ vector, we trivially obtain the corresponding state
vector realization. Hence, we concentrate, or profile, the state vector and optimize over the
model parameters via MCMC based estimation, using a chain of length 10,000, following
Chernozhukov and Hong (2004).

4.2. Estimation Results

490 As noted in Section 3, we follow a general-to-specific approach to estimation. Conse-
quently, model (3) is very richly parameterized, particularly regarding the specification of
the jump intensities. The idea is to allow for full generality and then eliminate the insignif-
icant features in the model. For brevity, we defer the estimation results for the general case
to the Supplementary Appendix. It turns out that the jump loading parameters, c_0^- , c_2^- ,
495 c_u^+ , are statistically insignificant, and the same applies for η . Hence, our more parsimonious

¹³Our specific weighting scheme stems from an analysis of the option pricing errors, showing that their
volatility is roughly linear in the level of market volatility.

model constrains these parameters to zero. For the negative jump intensity coefficients, this is readily interpreted. It implies that the frequency of jumps are governed exclusively by the level of the two factors, V_1 and U . The $\eta = 0$ and $c_u^+ = 0$ restrictions are more fundamental. First, $\eta = 0$ implies that U is a pure jump intensity factor which does not contribute directly to the diffusive volatility. This represents a major departure from existing continuous-time models, which are built from stochastic volatility factors.¹⁴ Second, the elimination of c_u^+ means that U is constrained to only affect the negative jumps. Again, this is an important departure from existing asset pricing models. These features are precluded in the typical approach to empirical option pricing, because the latter is built around multi-factor volatility models with a single (Gaussian) price jump component. These models rule out pure jump dynamic factors and do not allow for factors to impact the negative and positive jump intensities differentially. In our case, by letting the option panel determine the fit, we find the risk-neutral dynamics to involve a non-volatility factor that operates only on the negative jump intensity.

The estimation results for the general model (3) further reveal that the parameters controlling the risk-neutral law of U are not estimated very precisely. This result is largely due to the fact that the persistence of U is rather extreme with a half-life of approximately 8 years. With such a low degree of mean reversion, the parameters κ_u , μ_u and ρ_u cannot be recovered precisely as they play an insignificant role in determining the values of options with maturities of up to one year. A precise estimation of κ_u , μ_u and ρ_u requires far longer-dated options than available in our sample. This issue also arises in the analogous case of recovering the risk-neutral volatility parameters from options data if the volatility is very persistent, see, e.g., Broadie et al. (2007) and the references therein. Nonetheless, we have compelling evidence for the presence of U in the risk-neutral dynamics. First, note that the

¹⁴Instead, our specification shares critical features with the discrete-time GARCH type model of Christoffersen et al. (2012).

520 hypothesis that U is absent is a joint hypothesis that $\mu_u = 0$ as well as that the vector $\{U_t\}$ is not present, and such a hypothesis is strongly rejected by the data.¹⁵ Second, a constrained model in which U is absent performs significantly worse, both in- and out-of-sample, as documented in the Supplementary Appendix. Finally, even though the individual parameters κ_u , μ_u and ρ_u are poorly identified, the realizations of the tail factor U are well identified. 525 As discussed previously, the latter is crucial for our analysis of the risk-premium dynamics, as U represents the component of the left tail dynamics that is not tied to volatility.

The case of ρ_u is particularly interesting as this parameter is not endowed with a natural boundary condition that eliminates an associated feature from the model. Instead, it indicates the relative jump size in U stemming from (squared) co-price jumps versus a separate 530 source of jumps. As such, the parameter is restricted to the $[0, 1]$ interval, with the boundary values indicating either that U does not co-jump with the price process ($\rho_u = 0$) or that U is not subject to separate jump shocks ($\rho_u = 1$). Our estimation results suggest that ρ_u is sufficiently poorly identified that, at standard significance levels, we cannot rule out any value in $[0, 1]$. However, as we document below, ρ_u turns out to be largely irrelevant for the 535 extracted state vector realization throughout the sample.¹⁶ Thus, we only constrain ρ_u to fall within the unit interval.

We now turn to the results for the restricted model obtained after zeroing out c_0^- , c_2^- , c_u^+ and η .¹⁷ Table 4 reports the point estimates and associated standard errors. As expected, the volatility factors differ significantly in their degree of mean reversion, with V_2 having 540 a half life of about 5 months versus 3 weeks for V_1 . V_2 is also generally larger and has

¹⁵More formally, under the null that $\mu_u = 0$, the factor realization $\{U_t\}$ as well as the parameters κ_u and ρ_u are not identified, and hence testing such a hypothesis using a standard t-test (or Wald test) is invalid, see Andrews (2001).

¹⁶Specifically, we verify that imposing $\rho_u = 0$ or $\rho_u = 1$ has no material impact on any of our qualitative conclusions.

¹⁷A standard Wald test for the four parameters jointly taking the value of zero generates a p-value of 27.25%, confirming that we cannot reject this restriction at any standard level of significance.

a lower volatility-of-volatility coefficient than V_1 , implying we have a smaller and rapidly moving volatility factor and a larger, less volatile, but more persistent second volatility factor. Both display a strong negative association with the return innovations, generating an overall correlation between return and spot volatility innovations of around -0.95.¹⁸

Table 4: **Estimation Results**

Parameter	Estimate	Std.	Parameter	Estimate	Std.	Parameter	Estimate	Std.
ρ_1	-0.959	0.093	\bar{v}_2	0.010	0.000	c_0^+	0.372	0.029
\bar{v}_1	0.003	0.000	κ_2	1.864	0.103	c_1^-	111.061	4.446
κ_1	10.989	0.193	σ_2	0.170	0.006	c_1^+	25.855	4.971
σ_1	0.249	0.028	μ_u	7.124	24.096	c_2^+	81.719	6.947
μ_1	12.158	0.247	κ_u	0.0877	0.123	λ_-	25.944	0.196
ρ_2	-0.979	0.033	ρ_u	0.513	4.404	λ_+	36.620	0.857

Note: Parameter Estimates of Model (3). The model is estimated using S&P 500 equity-index option data sampled every Wednesday over the period January 1996-July 2010 and the parameters η , c_u^+ , c_0^- and c_2^- are all set to zero. Parameters are reported in annualized return units.

545 Turning to the left tail factor, we find U to have an estimated half-life of 8 years under the risk-neutral measure, thus far exceeding those of the volatility factors. Hence, this pure jump factor has the potential to impact the option prices substantially across both short and long maturities. Comparing our results with option-based estimation of multi-factor volatility models, reported in Bates (2000) and Christoffersen et al. (2009), we find that
550 the mean-reversion of the volatility in our model is far stronger than reported in the above-mentioned papers. This is “compensated” by the presence of the very persistent U factor. We recall that in the traditional volatility models, the left and right jump intensities are

¹⁸The value of this correlation coefficient varies with the relative size of the two factors. The reported value is obtained for the spot variances equaling their unconditional time series means. In light of the reported standard errors, this strongly negative coefficient is consistent with recent evidence exploiting an entirely different approach based on joint high-frequency data for volatility indices and underlying asset returns, see, e.g., Andersen et al. (2014).

proportional to the volatility factors. In our case, through the introduction of U , we drive a wedge between volatility and jump intensity and the option data identifies the latter as the more persistent one. Intuitively, since U controls the left jump tails, this result stems from the relative expensiveness of the OTM long maturity puts across our sample, i.e., the comparatively slow flattening out of the IV skew at long maturities.

5. Diagnostic of the Option Panel Fit and Model Performance

In this section, we explore whether model (3) provides a satisfactory characterization of the option surface dynamics. For this purpose, we first consider a sequence of more standard specifications as competitor models. They range from an extended version of the one-factor double-jump model of Duffie et al. (2000) to a model including three stochastic volatility factors. The one-factor model (1FGSJ) features square-root volatility, correlation between Gaussian return and exponential volatility co-jumps, and has a time-varying jump intensity given as an affine function of the volatility state. To allow additional flexibility, we also consider the two (stochastic volatility) factor version of the double-jump model, and we explore both a Gaussian (2FGSJ model) and a double-exponential (2FESJ model) jump distribution for the return jumps. Finally, we expand the most successful in-sample two-factor model into a three-factor return-volatility co-jump model (3FESJ-V) by introducing a third square-root volatility factor, thus expanding the number of factors in the traditional manner. The exact specifications for each of the alternative models and the corresponding in-sample parameter estimates and RMSE fit to the option panel are provided in the Supplementary Appendix. Generally speaking, they represent more elaborate specifications than estimated in the literature, and thus afford an improved in-sample fit to the option surface relative to many of the models considered in prior studies.

At this stage, we simply note that model (3) has a considerably lower overall RMSE to the option panel of 1.71% compared to RMSE values ranging from 3.14% for the one-

factor Gaussian double-jump model to 1.86% for the three-factor return-volatility co-jump model.¹⁹ Thus, model (3) provides a comparatively good fit to the surface. However, it is less evident whether this translates into an improved characterization of the key dynamic factors determining the evolution of, and associated risks related to, the IV surface as well as the corresponding risk premiums. To this end, in this section, we provide additional details concerning the model fit to the option characteristics as well as the fit to the nonparametric volatility estimates from high-frequency data. We conclude the section with various robustness checks.

5.1. State Vector Dynamics, Volatility Surface Dynamics, and Jump Intensities

We first analyze the state vector in our model. Table 5 reports summary statistics for the extracted time series of the three factors. We find that the jump volatility factor, V_1 , is the dominant component of the diffusive volatility under the physical probability measure, contributing roughly 2/3 to its total mean. The two volatility factors also exhibit some negative correlation (of order -0.3), while V_1 is only slightly less persistent than V_2 under the statistical measure. Next, the mean of U implies it contributes an average of 3.7 negative jumps per year to the negative jump intensity. Thus, given the average negative jump arrival of 5.6, U is the dominant driver of the negative jump tail. Moreover, the sample standard deviation of U indicates a substantial degree of variation over time, inducing significant fluctuations in the negative jump tail and the associated (high) price for market downside protection. In addition, we find that, also under \mathbb{P} , U is, by far, the most persistent of the three state variables. Finally, U exhibits nontrivial positive correlation with V_1 and slight negative correlation with V_2 . This is consistent with our risk-neutral model (3) in which V_1 and U are connected through the jumps and the feedback effect induced by the jump

¹⁹Using the asymptotic theory developed in Andersen et al. (2013), these differences in RMSE are highly statistically significant.

intensities of the two state variables.²⁰

	Summary statistics									
	Mean	Std	Skew	Kurt	AC(1)	AC(15)	AC(30)	Q(0.25)	Q(0.50)	Q(0.75)
V_1	0.017	0.035	5.037	36.687	0.884	0.250	-0.006	0.0001	0.0053	0.0162
V_2	0.012	0.009	0.737	3.363	0.840	0.369	0.102	0.0052	0.0103	0.0180
U	3.710	3.347	1.861	7.372	0.973	0.591	0.360	1.2538	2.8982	4.9409

Table 5: **Summary Statistics for the Recovered State Vector.** AC denotes autocorrelation and Q signifies quantile. Sample averages are for the period January 1996 - July 2010.

To gain further insight into the dynamics implied by the model estimates, on Figure 3, we plot the model-implied spot diffusive volatility, given by $\sqrt{V_1 + V_2}$, and the corresponding high-frequency nonparametric estimate in the upper panel, while the model-implied estimates of \sqrt{U} is depicted in the lower panel. The plots are intriguing along several dimensions. First, the option-implied estimate of the diffusive volatility has approximately the same sample mean as the nonparametric high-frequency estimate, but it is far less noisy, illustrating the potential gains from incorporating option information into volatility inference. Second, we notice spikes in market volatility and – even more strikingly – in U around well-known crises. Third, the negative jump intensity factor U portrays a very different picture than the diffusive volatility. For example, the peaks of U in the 1997 and 1998 crises as well as the European sovereign debt crisis match or exceed those observed from 2000 through 2003, yet the model-implied volatility is substantially higher in the latter than the former episodes. That is, the alternating shapes of the option surface signal that these events represent very different types of exposure to volatility and negative jump risks. Fourth, as expected, the financial crisis stands out from the rest. Moreover, the jump intensity factor U mean-reverts much slower than volatility following this crisis. The identical pattern is observed across all the episodes identified above in which the jump intensity rises strongly

²⁰However, Table 5 concerns the statistical measure while model (3) characterizes the risk-neutral measure. In general, no-arbitrage does not restrict the relation between the moments under the two measures.

relative to volatility. This implies that U contributes (relatively) more to the expensiveness
of OTM puts in the aftermaths of the Asian, Russian, and European crises than market
volatility. The opposite is true for the turbulent episodes surrounding 9-11 and the Second
Gulf War in 2002, where market volatility clearly is the dominant force. Likewise, the initial
spike in the jump intensity during the financial crisis was not caused solely by the U factor.
Instead, U is accountable for the subsequent slow mean reversion. Fifth, we notice that,
even during the quiet period 2004-2006, the negative jump intensity factor U remains at a
nontrivial level, implying approximately 1 jump per year.

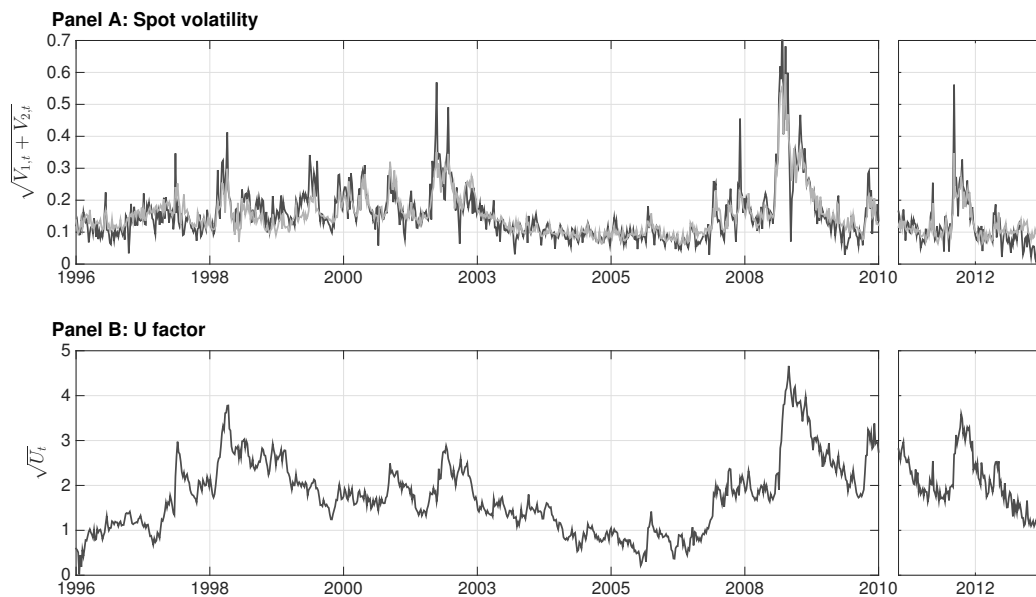


Figure 3: **Spot Volatility and the U Factor.** The top panel displays the spot diffusive volatility estimated from the high-frequency data (the dark line) and from the option panel (the light-colored line). The bottom panel displays the estimate of \sqrt{U} .

5.2. Fitting the Option Characteristics

Next we investigate the model's success in capturing the dynamics of the option panel. Recall from Section 2, that the first principal component of the option surface explains

630 more than 96% of the total variation, but the PCs fail to succinctly capture the dynamic dependencies of the option characteristics. The first principal component provides a fit (in RMSE) to the set of standardized options used in the PC analysis of 3.38%. We can compare this RMSE to the ones obtained by our parametric no-arbitrage models, reported in Table 6 below. Even, the simplest one-factor 1FGSJ model provides a significantly improved fit of 635 2.67% and this further drops to 1.40% for our preferred three-factor model. This is due to the nonlinear factor structure for the option panel implied by the parametric models (recall footnote 2). For the remainder of this section, we analyze the success of the parametric models in tracking the dynamics of the IV surface by focusing on their ability to fit the option characteristics.

640 On Figure 4 we plot the characteristics along with the model-implied fit. Perhaps not surprisingly, the model provides a near perfect fit to the IV level, both for periods of turmoil and relative tranquility. The fit to the IV skew is also quite satisfactory, although the model slightly overestimates the skew during 1999 and tends to underestimate it at peaks of financial crises. Nonetheless, there is no evidence of major systematic biases and the 645 relative errors are small except for the Fall of 2008.²¹ Turning to the IV term structure, we observe, from the top right panel of Figure 4, that our model provides an almost perfect fit to this characteristic. Finally, the most challenging feature of the surface is the IV skew term structure. Nonetheless, the model fits this feature well except for two noticeable periods, namely the aftermaths of the 1998 Russian crises and the recent financial crisis. During 650 these episodes, our model predicts a somewhat steeper IV skew term structure than actually

²¹Our finding of underestimation of the skew during highly turbulent periods is consistent with recent nonparametric evidence in Bollerslev and Todorov (2013) of time-variation in the shape of the jump tails. Accounting for such feature of the data will alleviate the slight mispricing during such periods, observed on Figure 1, but it will take us outside the tractable generalized affine framework. Note that some of the time variation in the shape of jump tails can be partially offset by very high values of the U factor, as the latter is not constrained to be part of volatility. Furthermore, the measurement errors in the option prices during crises periods are exceptionally large, so gauging model quality by the size of the pricing errors during these periods is potentially misleading.

observed. Intuitively, this is indicative of negative jump tails that need to be even more persistent, during these two periods, than the model implies to deliver the slower thinning of the risk-neutral tails along the maturity dimension of the conditional return distribution.

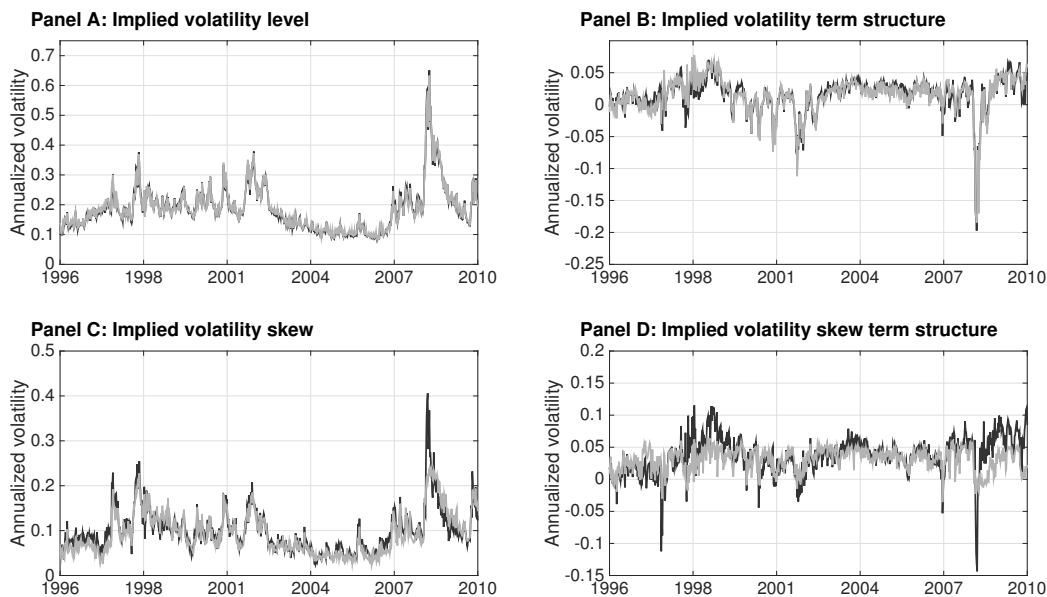


Figure 4: **The Model-Implied Fit to the Option Characteristics.** The dark line corresponds to the data and the light-colored line refers to the fit by model (3).

To benchmark the success of our model (3) in capturing the option surface characteristics, we now compare it to the fit provided by the alternative stochastic volatility models discussed at the beginning of this section. The results are presented in Table 6. We stress that our estimation does not minimize the distance between the observed and model-implied option characteristics. Nevertheless, our model provides a superior fit to each of the four option characteristics. The improvement is quite significant compared to one- and two-factor models with Gaussian price jumps. Moreover, the improved fit offered by our model is not solely attributable to the addition of an extra factor. Indeed, the alternative three-factor model performs significantly worse at fitting the term structure of the IV level and skew.

Furthermore, removing U (leading to the model 2FESJ) produces a significant deterioration in the fit to the IV skew. Finally, our model improves substantially on 1FGSJ and 2FGSJ models in fitting the spot volatility and is essentially on par with the rest of the alternative specifications in this regard.

	Model Fit				
	1FGSJ	2FGSJ	2FESJ	3FESJ-V	3F
IV Level	1.73	1.01	0.88	0.68	0.64
IV Term Structure	2.72	1.42	1.06	1.30	0.86
IV Skew	3.81	2.88	2.54	2.13	1.96
IV Skew Term Structure	2.79	3.70	2.01	2.57	2.40
Spot Volatility	5.199	4.130	3.944	3.945	3.977
Options with Fixed m, τ	2.67	2.10	1.89	1.58	1.40
All Options	3.14	2.56	2.07	1.86	1.71

Table 6: **Fit to Options, Characteristics and Spot Volatility.** The numbers in the table are the RMSEs (in percent) from fitting the IV surface characteristics (first four rows), the spot volatility (fifth row), the implied volatilities for fixed moneyness $m \in \{-4, -3, -2, -1, -0, 1, 2\}$ and tenor $\tau \in \{0.1, 0.3, 0.8\}$ (sixth row), and all options used in the estimation (seventh row). The models in the comparison are defined as follows. 1FGSJ (2FGSJ) refer to the One (Two) Factor Gaussian Jump model with time-varying jump intensity; 2FESJ refers to the Two-factor Exponential jump model with time-varying jump intensity; 3FESJ-V refers to the Three-Factor Exponential jump model with time-varying jump intensity; 3F refers to the Three-factor Exponential jump model with the separate jump factor, U in equation (3). All models are explicitly defined in the Supplementary Appendix.

The distinguishing feature of model (3) is the presence of U which resides only in the negative risk-neutral jump intensity. We now explore the specific role of U in driving the surface dynamics. To this end, on Figure 5, we plot the fitted IV surface characteristics as well as their sensitivity with respect to U at the current values of the state vector for each day in the sample. These sensitivities are measured via the change of the characteristics stemming from increases and decreases in U by 50% from its estimated value. For the IV level, U has a limited impact except for crises periods when volatility is very high. This is to be expected as short-term ATM IV is primarily determined by the level of the diffusive volatility (recall, U is absent from the latter). On the other hand, U has a very pronounced and more uniform impact on the IV skew. That is, the significance of U for the skew is

ubiquitous and remains nontrivial, even during the tranquil period of 2004-2006. Turning to the IV term structure in the top right panel of Figure 5, we observe strong time-variation in the impact of U , with the effect being most substantial following the Asian, Russian and recent Financial crises. In contrast, U has a very limited effect on the IV term structure during 2004-2006. This is not surprising. The intensity of the volatility jumps in model (3) depends on U . Hence, a higher value of U today triggers higher expected future diffusive volatility, and given the persistence of U under \mathbb{Q} , this effect is long-lasting and tends to elevate the IV term structure following the crises of 1997, 1998 and 2008. Finally, U has a relatively small impact on the IV skew term structure, except when U is very high. Overall, Figure 5 documents that U has a significant impact on both the term structure and the skew. The impact on the skew is largely immune to the state of the system, while the impact on the term structure is concentrated in extended periods following some of the crises in the sample. This effect of U on the surface helps account for the dynamic interdependencies among the characteristics documented in Section 2.

5.3. Robustness of Estimation Results and Inference

We next explore the robustness of our empirical findings. First, we check the sensitivity with respect to the penalization term for the volatility fit in the objective function. We vary λ around the original choice of 0.2 by 50% in either direction. It is useful when interpreting the results below to keep in mind that a misspecified model will face tension in simultaneously fitting the option surface and matching the high-frequency based estimate of spot volatility. The results are reported in the Supplementary Appendix. We note the remarkable stability of the parameters with the exception of σ_2 and c_0^+ for which the changes are somewhat large compared with the precision in their recovery. Hence, there is some evidence for misspecification, but the critical features of the system remain virtually unchanged. Most significantly, the extracted tail factor U is unaffected which is crucial for our analysis of the

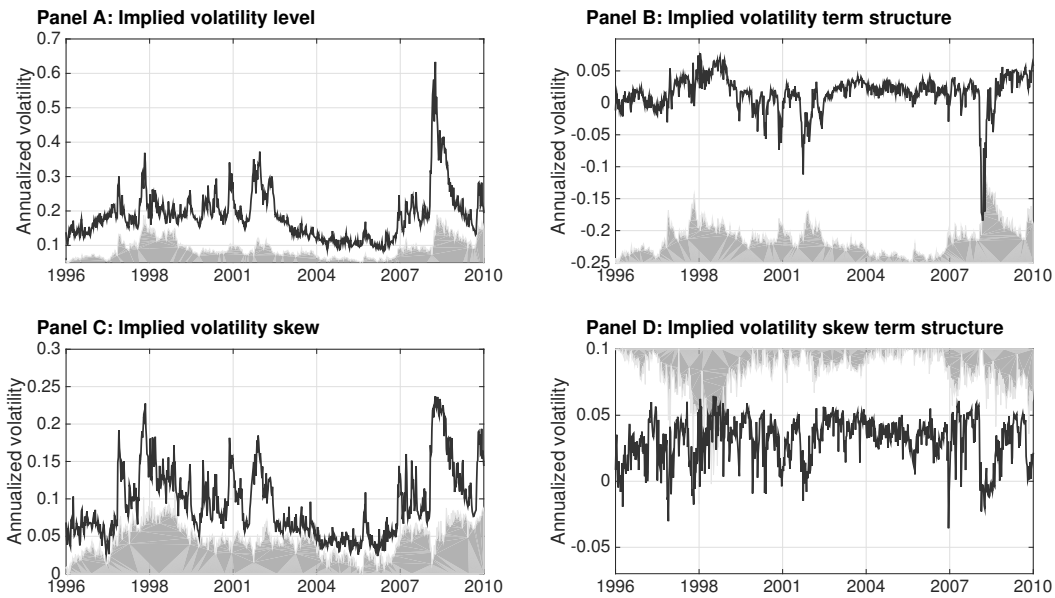


Figure 5: **The effect of U on the Option Characteristics.** The line corresponds to the fitted characteristics and the shaded area indicates the change in the characteristics stemming from a decrease versus an increase in U by 50% relative to the current estimated value. To better capture the effect of U on the option characteristics, we use only the days in the sample for which the shortest maturity of the options is less than 10 business days in the computation of the shaded area.

risk premium dynamics later on.

Second, the Supplementary Appendix reports results for subsample estimation covering 1996-2006 and 2007-2010. The fit is excellent for the longer 1996-2006 subsample, with an overall RMSE of 0.99%. While this sample excludes the financial crisis, and thus poses less of a challenge to the option pricing model, the sample still covers some dramatic episodes around 1997, 1998 and the internet bubble, along with some extremely low volatility levels during 2004-2006. The shorter and extremely turbulent 2007-2010 period is much harder to accommodate, and the RMSE is now 2.16%. We do observe some degree of parameter instability, mainly impacting the risk-neutral means of the two volatility factors, \bar{v}_1 and \bar{v}_2 , which tend to move in opposite directions, as well as the loadings on the volatility factors in the jump intensities. This is indicative of some misspecification in the modeling of diffusive volatility. Nonetheless, the parameters λ^- and λ^+ , governing the jump tail decays, are remarkably stable across subsamples. Likewise, the estimates of μ_1 , controlling the volatility jumps, are stable. And most importantly for our analysis, the extracted realization of U , across the entire sample, remain near invariant regardless of whether the full sample or subsample parameter estimates are employed.

6. Out-of-Sample Performance

Our model (3) is quite richly parameterized, containing three state variables along with the 18 separate parameters reported in Table 4. This may raise concerns regarding potential in-sample overfitting. We address this issue by exploring the out-of-sample performance vis-a-vis the more parsimoniously parameterized alternatives introduced previously in Section 5. If the dynamic features extracted from the option surface through model (3) are genuine and stable, the model should continue to provide a superior fit also for the options observed beyond the in-sample period.

To assess the robustness of model (3) relative to the alternative specifications, we use

the parameters for each model estimated over the period January 1st 1996 - July 21st 2010 to price the options week-by-week over the subsequent period from July 22nd 2010 to April 23rd 2013, using the criterion function from equation (9), but optimizing only over the state vector. This out-of-sample period contains quotes for over 100,000 separate options, representing more than 56% of the number of in-sample observations.²² The average IV (across all options) in the out-of-sample period equals 24.17%, while the average ATM IV is 18.40%.

From Figure 3, we note that spot volatility filtered from model (3) in the out-of-sample period continues to provide an excellent fit to the spot volatility estimated from high-frequency returns. Thus, effectively, we decompose the factors governing the option surface into current spot volatility and a separate left jump tail factor, U . The extracted volatility states provide an excellent basis for forecasting future realized return volatility and jumps, thus freeing U to accommodate the portion of the risk premium dynamics that is not tightly related to the volatility states.

The out-of-sample fit to the option surface for the various models are summarized in Table 7. Panel A provides the overall root-mean-squared error (RMSE) and Panel B indicates the performance for specific regions of the surface. On the right in Panel B, the RMSE for model (3) is given, while the remaining entries provide the percentage *excess* RMSE of the alternative specifications relative to model (3). Thus, positive entries signify the degree to which the models perform worse than model (3) for that part of the option surface during the out-of-sample period.

²²The sharp increase to over 700 quotes per day for the out-of-sample analysis is due to two factors. One, there are more options quoted at a given tenor - thus filling gaps in the moneyness dimension. Two, the introduction of weekly options increases the number of tenors available on each day - thus enriching the data in the maturity dimension. Weekly options were introduced in 2005, but only by 2011 did the associated volume become a significant fraction (almost 20%) of the total trading volume for SPX options. As a reference, for January 1996 – December 1998, we have 158 contracts per day, while we have 490 contracts per day between January 2008 and July 2010.

The results are striking. The superiority of model (3) is more pronounced out-of-sample than in-sample. Moreover, we see that the exponential specification for return jumps performs significantly better than the Gaussian, while two-factor models offer nontrivial improvements over one-factor representations. However, none of these more standard specifications come close to matching the performance of model (3). Furthermore, we observe that the traditional three-factor stochastic volatility model performs comparatively poorly out-of-sample, with the two-factor model doing equally well or slightly better, reflecting some degree of in-sample overfit for the former model. Thus, in fact, there is a danger of over-parameterizing the in-sample specification, but this does not manifest itself for model (3). Moving to the individual regions of the surface, Panel B documents that model (3) outperforms every other model for each single region of the surface, so the superior out-of-sample fit is uniform. Finally, in Panel C we observe that we fit, out-of-sample, the spot volatility far better than any of the alternative models. We conclude that the risk-neutral dynamics obtained from the in-sample period remains stable and continue to capture the salient features of the option surface dynamics beyond the estimation period.

To illustrate the type of scenarios for which the improvement of model (3) relative to the more standard one-factor Gaussian jump model, 1FGSJ, is particularly significant, Figure 6 depicts the fit of the two models to the IV skew and term structure on two separate trading days. December 19, 2012, represents a fairly typical day with an about average skew and term structure. For this day, the fit of either model is quite satisfactory, and there is no major discrepancy between the two. In contrast, for September 8, 2010, the skew is elevated although the level of volatility is moderate. It represents a quite common occurrence in the aftermath of turbulent market conditions – in this case associated with the initial European sovereign debt crisis. On this date, the one-factor model misses the ATM IV level quite badly, and it provides a very poor fit to the term structure. The problem is that the steep skew only can be accommodated through a high jump intensity which, in the standard model, is

Panel A: Overall Option RMSE											
	1FGSJ		2FGSJ		2FESJ		3FESJ-V		3F		
	RMSE		RMSE		RMSE		RMSE		RMSE		
	3.28		2.66		2.25		2.26		1.77		
Panel B: Sorting by Moneyness and Maturity											
	1FGSJ		2FGSJ		2FESJ		3FESJ-V		3F		
	RRMSE		RRMSE		RRMSE		RRMSE		RMSE		
τ	≤ 60	> 60									
$m \leq -3$	0.68	1.16	0.60	0.48	0.09	0.33	0.14	0.30	2.28	2.76	
$-3 < m \leq -1$	0.49	0.71	0.32	0.34	0.14	0.33	0.03	0.47	1.53	1.95	
$-1 < m \leq 1$	1.43	0.39	0.99	0.30	0.74	0.08	0.67	0.16	0.91	1.36	
$m > 1$	1.77	0.70	0.89	0.38	0.98	0.15	0.82	0.07	1.24	1.86	
Panel C: Spot Volatility RMSE											
	1FGSJ		2FGSJ		2FESJ		3FESJ-V		3F		
	RMSE		RMSE		RMSE		RMSE		RMSE		
	6.23		5.01		4.05		4.27		3.82		

Table 7: **Out-of-sample Option Pricing Performance and Volatility Fit.** We report RMSEs in implied volatility (in percent). The abbreviations for the different models are as in Table 6. RRMSE is the ratio of the RMSE of a given model over that of the 3F model minus one.

only feasible if volatility is high. Hence, the fit to the ATM volatility is sacrificed in order
775 to fit the OTM put options. Moreover, at an elevated volatility level, the mean-reversion
in volatility prevents the term structure from being sufficiently steep.²³ In contrast, with
the flexibility afforded by U , model (3) can readily accommodate a persistent state with an
elevated intensity for the left jump tail. Furthermore, the cross-excitation between jumps
and volatility is sufficient to generate an increase in the expected return variation over time,
780 thus adapting to the relatively steep slope of the term structure.

The key to the success of our model is the severance of the linkage between jump intensity
and volatility which is, a priori, imposed in most prior work, as discussed in Section 3. In
using standard models for the analysis of risk premia, one will inevitably treat the systematic
mispricing of the IV skew and term structure, documented in the bottom panels of Figure 6,

²³We have confirmed that identical problems plague, e.g., the 2FESJ model in this type of scenario.

785 as persistent observation error. This problem is recurring. Throughout the in-sample period, we observe similar qualitative developments following the Asian and Russian crises, and the 2008-2009 financial crisis, while for the out-of-sample period, the second round of the European debt crisis in late 2011 also generates this type of persistent dynamic in the surface. Hence, using the standard modeling framework will induce systematic biases in the inference
790 for risk premia.

7. Risk Premia Dynamics and Predictability

This section relates our findings based on the option panel to the underlying return data. In particular, we study the links between the state vector, or risk factors, extracted from the option panel and the volatility and jump risks inferred from the underlying stock
795 returns. This sets the stage for direct exploration of the equity and variance risk premiums and their association with the option-implied factors. Given our analysis, we rely on model (3) for tracking the IV surface dynamics. We continue to avoid making strong assumptions regarding the evolution of the actual market risks. Consequently, this part of our analysis is fully nonparametric, and we invoke only minimal stationarity conditions regarding the
800 \mathbb{P} -law.

7.1. Connecting the Information in the Option Panel and the Underlying Asset

To define risk premia, we must develop consistent notation concerning the pricing of each source of risk in model (3). We define,

$$\begin{aligned} W_{1,t}^{\mathbb{P}} &= W_{1,t}^{\mathbb{Q}} - \int_0^t \lambda_s^{W_1} ds, & W_{2,t}^{\mathbb{P}} &= W_{2,t}^{\mathbb{Q}} - \int_0^t \lambda_s^{W_2} ds, \\ B_{1,t}^{\mathbb{P}} &= B_{1,t}^{\mathbb{Q}} - \int_0^t \lambda_s^{B_1} ds, & B_{2,t}^{\mathbb{P}} &= B_{2,t}^{\mathbb{Q}} - \int_0^t \lambda_s^{B_2} ds, \end{aligned} \tag{10}$$

where $W_{1,t}^{\mathbb{P}}$, $W_{2,t}^{\mathbb{P}}$, $B_{1,t}^{\mathbb{P}}$ and $B_{2,t}^{\mathbb{P}}$ are \mathbb{P} Brownian motions and $\lambda_t^{W_1}$, $\lambda_t^{W_2}$, $\lambda_t^{B_1}$ and $\lambda_t^{B_2}$ denote
805 the associated prices of risk. The compensator of the jump measure, μ , under the \mathbb{P} measure

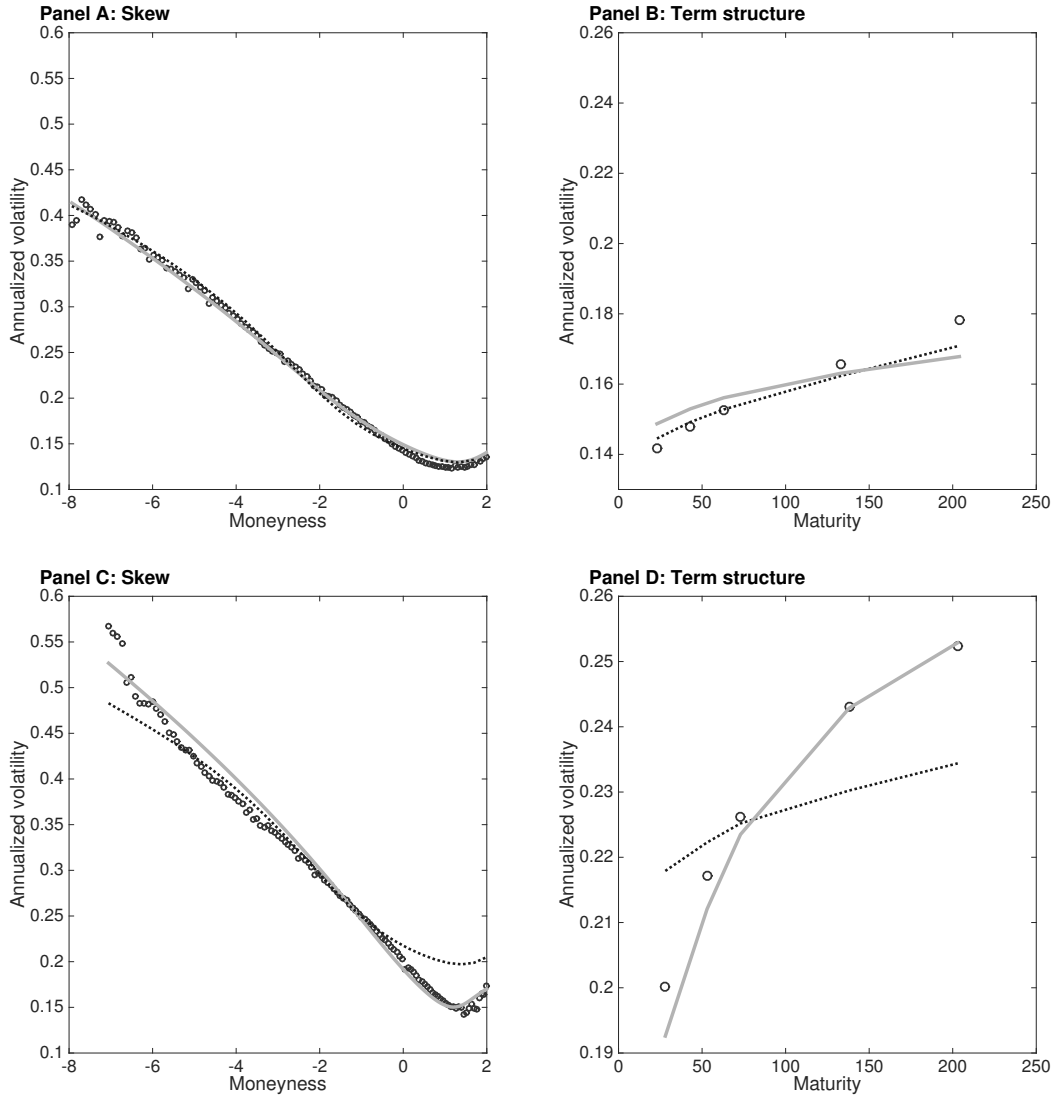


Figure 6: **Out-of-sample Fit to IV Skew and Term Structure.** The figure plots the fit to the IV skew and term structure for the trading days December 19, 2012 (upper row) and September 8, 2010 (bottom row). The circles represent the observed Black-Scholes implied volatilities; the continuous line is the fit from model 3F; the dashed line is the fit from model 1FGSJ.

is given by $dt \otimes \nu_t^{\mathbb{P}}(dx, dy)$, and the mapping $\nu_t^{\mathbb{P}}(dx, dy) \rightarrow \nu_t^{\mathbb{Q}}(dx, dy)$, defined for every jump size x and y and every point in time t , reflects the compensation for jump risk.

The dynamics of the stock price process under the physical probability measure \mathbb{P} is then,

$$\frac{dX_t}{X_{t-}} = \alpha_t dt + \sqrt{V_{1,t}} dW_{1,t}^{\mathbb{P}} + \sqrt{V_{2,t}} dW_{2,t}^{\mathbb{P}} + \int_{\mathbb{R}^2} (e^x - 1) \tilde{\mu}^{\mathbb{P}}(dt, dx, dy), \quad (11)$$

where

$$\alpha_t - (r_t - \delta_t) = \lambda_t^{W_1} \sqrt{V_{1,t}} + \lambda_t^{W_2} \sqrt{V_{2,t}} + \int_{\mathbb{R}^2} (e^x - 1) \nu_t^{\mathbb{P}}(dx, dy) - \int_{\mathbb{R}^2} (e^x - 1) \nu_t^{\mathbb{Q}}(dx, dy), \quad (12)$$

810 is the spot equity risk premium, reflecting compensation for diffusive and (price) jump risks.

The conditional cum-dividend equity risk premium over the horizon τ is thus given by,²⁴

$$\text{ERP}_t^\tau \equiv \frac{1}{\tau} \mathbb{E}_t^{\mathbb{P}} \left(\int_t^{t+\tau} (\alpha_s - (r_s - \delta_s)) ds \right). \quad (13)$$

We next define the quadratic variation over $[t, t+\tau]$ which we denote $QV_{t,t+\tau}$. It captures the return variation over the given horizon and is given by,

$$\begin{aligned} QV_{t,t+\tau} &= QV_{t,t+\tau}^c + QV_{t,t+\tau}^j, \\ QV_{t,t+\tau}^c &= \int_t^{t+\tau} (V_{1,s} + V_{2,s}) ds, \quad QV_{t,t+\tau}^j = \int_t^{t+\tau} \int_{\mathbb{R}^2} x^2 \mu(ds, dx, dy), \end{aligned} \quad (14)$$

where we decompose the return variation into terms generated by the continuous and jump
815 component of X , $QV_{t,t+\tau}^c$ and $QV_{t,t+\tau}^j$. Further, note that the quadratic variation is inde-

²⁴Notice that since a long position in the market index involves a commitment of capital, a part of the wedge in the \mathbb{P} and \mathbb{Q} expectations of the cum-dividend equity returns reflects compensation for the time-variation in the risk-free rate. This term is, of course, absent if we instead define the equity risk premium using futures on the market index.

pendent of the probability measure. The variance risk premium is defined as,

$$\text{VRP}_t^\tau \equiv \frac{1}{\tau} \left[\mathbb{E}_t^{\mathbb{P}}(QV_{t,t+\tau}) - \mathbb{E}_t^{\mathbb{Q}}(QV_{t,t+\tau}) \right], \quad (15)$$

and is compensation for the variance risk in X .

We are also interested in assessing directly the risks and risk premiums associated with jumps. In particular, we want to gauge the compensation for large price jumps and to
 820 allow for a separate risk premium for the negative versus positive jumps. We obtain direct measures of the jump risks by simply counting the number of “big” jumps over the relevant horizon,

$$LT_{t,t+\tau}^K \equiv \int_t^{t+\tau} \int_{\mathbb{R}^2} 1_{\{x \leq -K\}} \mu(ds, dx, dy), \quad RT_{t,t+\tau}^K \equiv \int_t^{t+\tau} \int_{\mathbb{R}^2} 1_{\{x \geq K\}} \mu(ds, dx, dy), \quad (16)$$

where K is a prespecified threshold. We set $K = 0.5\%$ in the subsequent analysis.²⁵

The risk measures we have introduced, including $QV_{t,t+\tau}^c$, $QV_{t,t+\tau}^j$, $LT_{t,t+\tau}^K$ and $RT_{t,t+\tau}^K$, are
 825 not directly observable, but we can estimate them using high-frequency and overnight futures returns. Naturally, since intraday data are available only during active trading, our high-frequency measures pertain exclusively to the trading intervals within $[t, t + \tau]$. We denote the latter with superscript i (for *intraday* based measures), e.g., $QV_{t,t+\tau}^i = \sum_{s=t}^{t-1+\tau} QV_{s+\pi, s+1}$, where π denotes the fraction of the day corresponding to the overnight period, and $1 - \pi$
 830 indicates the length of the trading day. $QV_{t,t+\tau}^{c,i}$, $QV_{t,t+\tau}^{j,i}$, $LT_{t,t+\tau}^{K,i}$ and $RT_{t,t+\tau}^{K,i}$ are defined analogously. By now, there are standard methods for constructing estimates for these risk measures as well as the corresponding equity and variance risk premia. We provide the details regarding our empirical implementation in the Appendix.

²⁵This (fixed) threshold K is large enough that we can separate returns exceeding this (absolute) level from diffusive volatility using 1-minute observations. Experiments with alternative cutoffs produced similar results.

7.2. The Predictability of Equity and Variance Risk and Risk Premia

835 We now explore the relationship between the option-implied factors, V_1 , V_2 and U , driving the option surface dynamics, and the various risk measures and risk premia associated with the underlying asset. We rely on alternative versions of the following predictive regression,

$$y_t = \alpha_0 + \alpha_1 V_{1,t} + \alpha_2 V_{2,t} + \alpha_3 U_t + \epsilon_t, \quad (17)$$

where the left hand side represents, in turn, the empirical jump and diffusive variance risk measures and the risk premia, i.e., $y_t = \widehat{LT}_{t,t+\tau}^{K,i}$, $\widehat{RT}_{t,t+\tau}^{K,i}$, $\widehat{QV}_{t,t+\tau}^{c,i}$, $\widehat{QV}_{t,t+\tau}$, $\log\left(\frac{X_{t+\tau}}{X_t}\right) - \frac{1}{\tau} \int_t^{t+\tau} (r_s - \delta_s) ds$ and \widehat{VRP}_t^τ . Given the relationships explicated in Section Appendix B of the Appendix, it is evident that the regressions based on the alternative y_t variables, asymptotically in sample size, yield estimates identical to those based on the corresponding infeasible measures of interest, i.e., $\sum_{s=t}^{t-1+\tau} \int_{s+\pi}^{s+1} \int_{\mathbb{R}} 1_{\{x \leq -K\}} \nu_s^{\mathbb{P}}(dx, dy)$, $\sum_{s=t}^{t-1+\tau} \int_{s+\pi}^{s+1} \int_{\mathbb{R}} 1_{\{x \geq K\}} \nu_s^{\mathbb{P}}(dx, dy)$, $QV_{t,t+\tau}^{c,i}$, $QV_{t,t+\tau}$, ERP_t^τ and VRP_t^τ . Thus, the predictive regression in equation (17) speaks
845 directly to the linkages between the option surface dynamics and the risks and risk premia associated with the equity index.

In general, if the premia for the diffusive and jump risks are spanned by the factors V_1 , V_2 and U , then the expectation of y_t conditional on time t information will be functionally related to $V_{1,t}$, $V_{2,t}$ and U_t . Moreover, in the standard case, almost universally adopted
850 in option pricing applications, the measure change preserves the affine structure, so the conditional mean of y_t is linear in $V_{1,t}$, $V_{2,t}$ and U_t . Hence, the regression in equation (17) produces optimal (mean-square error) predictors for the volatility and jump risks at time t . Furthermore, conceptually, our extraction of $V_{1,t}$, $V_{2,t}$ and U_t provides a richer information set for forecasting the volatility and jump realizations than the history of underlying asset
855 returns. The latter, at best, generates estimates of the path for $\{V_{1,s} + V_{2,s}\}_{s \leq t}$ as well as associated jump variation measures.

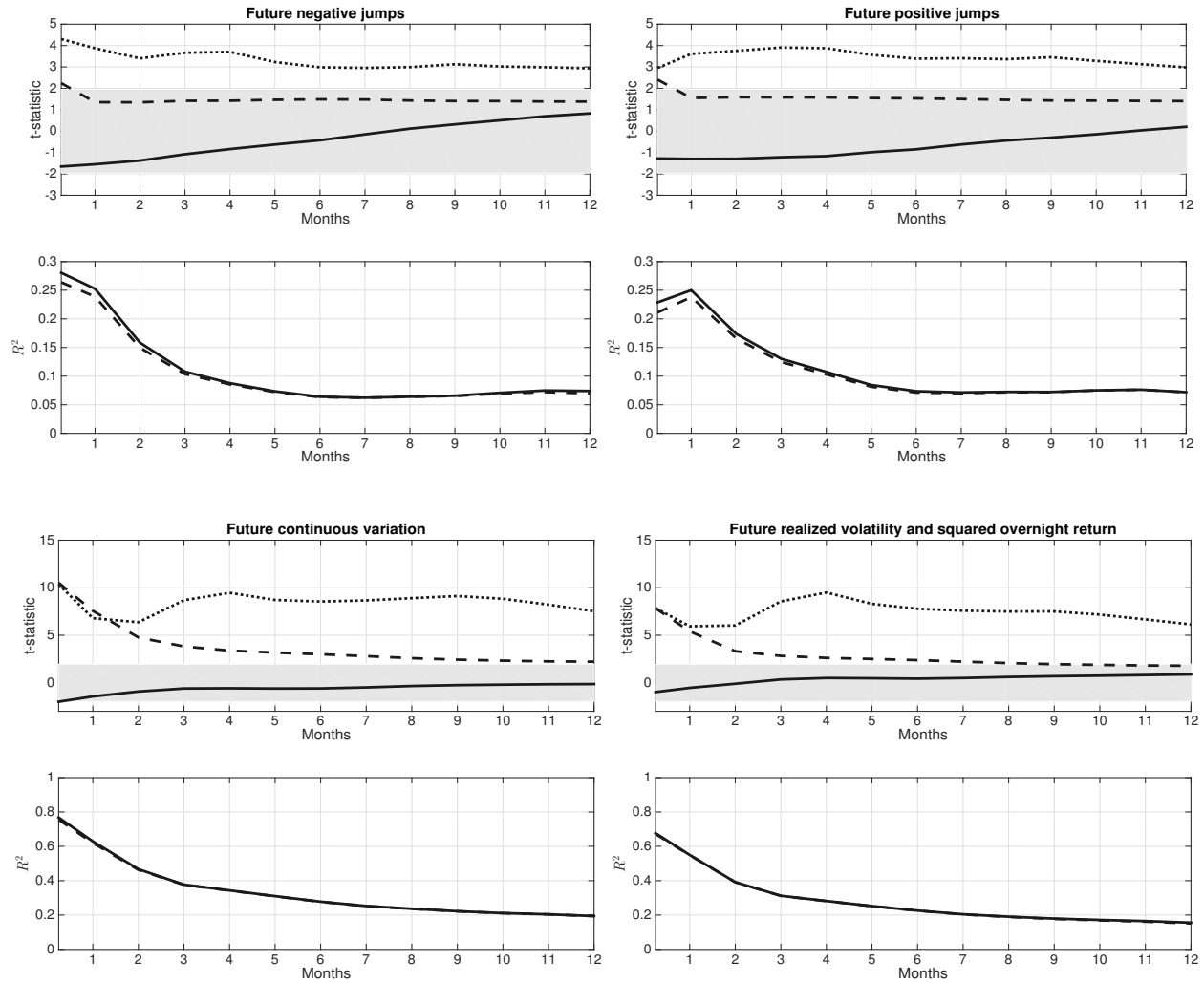


Figure 7: **Predictive Regressions for Volatility and Jump Risks.** The volatility and jump risk measures are defined in (A.2)-(A.3). For each regression, the top panels depict the t-statistics for the individual parameter estimates while the bottom panels indicate the regression R^2 . The predictive variables are V_1 (dashed-dotted line), V_2 (dashed line) and \tilde{U} (solid line), where \tilde{U} is the residual from the linear projection of U on V_1 and V_2 . The regression standard errors are constructed to also account for the estimation error in the projection generating \tilde{U} . The dashed lines in the R^2 plots correspond to constrained regressions, including only V_1 and V_2 .

We summarize the results from the predictive regressions in Figures 7 and 8. Since we are particularly interested in the incremental role of the novel factor U , we initially project U linearly onto the two volatility factors and denote the residual by \tilde{U} . Consequently, \tilde{U} reflects
860 the features of the system not associated with the traditional volatility factors. Given our

relatively short sample, we compute the predictive regressions for horizons up to one year only. Figure 7 shows that the state variables, extracted from the option panel, have significant explanatory power for the future evolution of risks. In particular, the plot pertaining to the count of positive and negative jumps reveals that the jump intensities display highly predictable time-variation under the statistical measure, \mathbb{P} , i.e., $\nu_t^{\mathbb{P}}(dx, dy)$ is truly a function of t . Moreover, the state variables differ greatly in their ability to forecast the future volatility and jump intensity. Specifically, once we control for the volatility factors, \tilde{U} provides no incremental explanatory power. This is evident both from the insignificant t -statistics corresponding to \tilde{U} and the trivial drop in R^2 when we exclude \tilde{U} from the regressions. Hence, Figure 7 is consistent with a model for which the jump intensity, under \mathbb{P} , depends only on the volatility factors V_1 and V_2 , but not \tilde{U} .²⁶ Finally, since the empirical detection of jumps inevitably is subject to some degree of measurement error and literally is infeasible during the overnight period, we also display the predictability regarding the combined quadratic return variation. Since the jump and overnight return variation is less predictable, the overall explanatory power drops slightly relative to the results for the continuous variation, but the qualitative pattern is identical. In short, the distinct return variation components are highly predictable, yet the forecast power of \tilde{U} is insignificant across all alternative constellations. Of course, the lack of statistical significance does not imply that U has no impact on the \mathbb{P} dynamics of volatility and jump risks, but rather that the effect is marginal compared to that of the volatility factors.

We now turn to the predictability of the equity and variance risk premia. Figure 8 indicates that our three factors, extracted from the option panel, now take on very different roles. In particular, a significant part of the predictability of both the equity and variance

²⁶In general, since V_1 contains jumps of time-varying intensity that load on all the factors, V_1 , V_2 and U , the conditional forecast of future volatility $V_{1,t} + V_{2,t}$ still depends (critically) on the current value of the third factor U .

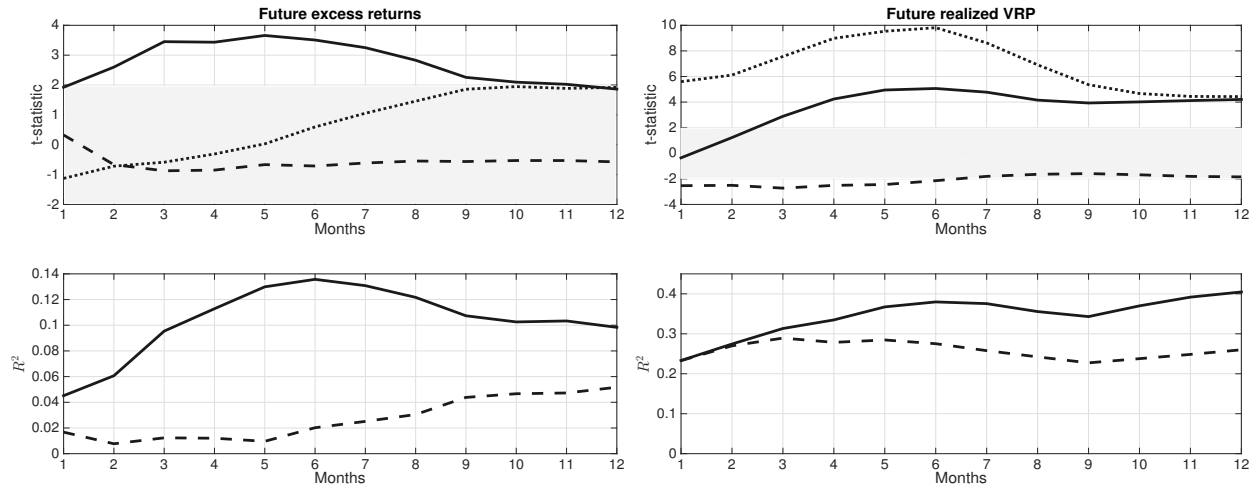


Figure 8: **Predictive Regressions for Equity and Variance Risk Premia.** For each regression, the top panels depict the t-statistics for the individual parameter estimates while the bottom panels indicate the regression R^2 . The predictive variables are V_1 (dashed-dotted line), V_2 (dashed line) and \tilde{U} (solid line), where \tilde{U} is the residual from the linear projection of U on V_1 and V_2 . The regression standard errors are constructed to also account for the estimation error in the projection generating \tilde{U} . The dashed lines in the R^2 plots correspond to constrained regressions, including only V_1 and V_2 .

risk premia is due to the U factor. For the variance risk premia, V_1 also contributes strongly
885 at shorter horizons, while, importantly, for the equity risk premium \tilde{U} is the single dominant
explanatory factor for all horizons. The importance of U for predicting both the equity and
variance risk premia is consistent with Bollerslev and Todorov (2011) who find the equity
and variance risk premia to embed a common component stemming from compensation of
left jump tail risk. The fact that both the equity and variance risk premia depend on U ,
890 coupled with the significant persistence of the latter, rationalizes the predictive power of
the variance risk premium for future excess returns, documented in Bollerslev et al. (2009)
and Drechsler and Yaron (2011). The limited role for the two volatility factors mirrors the
conclusions of many prior studies on the risk-return tradeoff, going back to, e.g., French et al.
(1987) and Glosten et al. (1993). Finally, we note that our results are not driven by the
895 events surrounding the financial crisis. Qualitatively identical results apply for subsamples

that end prior to 2007.²⁷

Another way to gauge the importance of U , and proper model specification in general, for predicting the equity and variance risk premia is to contrast our evidence above to findings generated by standard jump-diffusive models. Since the results are entirely consistent with our prior conclusions, we briefly summarize the results and refer to the Supplementary Appendix for details. If we omit U from the model, we are still left with an elaborate model which, besides the two volatility state variables driving the dynamics of the option surface, incorporates both diffusive and jump leverage effects, co-jumps in returns and volatility, and separate decay rates for the left and right (exponential) jump tails.²⁸ We find that the forecast performance regarding the future evolution of volatility and jump risks is similar to the corresponding results in Figure 7. Given that \tilde{U} plays only a minimal role in forecasting these quantities within model (3), this is quite intuitive. Moreover, as before, when considering the equity risk premium, the volatility factors are largely insignificant (and as likely to be negative as positive), and the R^2 of the predictive regression for the future excess returns is dramatically reduced. In short, the evidence for predictability of the equity risk premium vanishes when the option surface dynamics is modeled in the common jump-diffusive framework, and driven exclusively by volatility factors. Hence, the inclusion of the U factor, allowing for the left risk-neutral tail to have a separate source of variation, is pivotal for capturing the predictability in the equity risk premium. Finally, for the variance risk premium, both volatility factors are significant in the two-factor model, but the R^2 of the variance risk premium regression is notably lower than for our three-factor model (3).

To summarize, consistent with prior findings, we document a substantial time variation in the pricing of market risks. However, in a key departure from existing work, we provide strong evidence that the factors driving risks and risk premia differ in a systematic way. This

²⁷The documentation of these results are available upon request.

²⁸The corresponding two-factor model with Gaussian jumps performs less well along all dimensions.

920 is ruled out, a priori, through the structure preserving measure transformations adopted in most prior option pricing studies. Thus, our results point towards the importance of allowing for nonlinearities in the pricing kernel and have implications for the ability of structural economic models to rationalize the predictability of the equity and variance risk premia. We discuss this next.

925 7.3. Structural Implications of the Predictive Power of the Option Surface

Figures 7 and 8 demonstrate that the factor U , driving a substantial part of the OTM short maturity put option dynamics, has no impact on the *actual* volatility and jump dynamics of the underlying asset. In contrast, the factor has a critical effect on the *pricing* of volatility and jump risk. In other words, it resembles a risk premium and not a risk factor. Can we rationalize this finding from an economic perspective? To guide intuition, we compare the findings in Figures 7 and 8 with those from recent structural models that link option prices to fundamental macroeconomic risks, such as aggregate consumption and dividends. This emerging literature has made important progress in tackling the challenging, yet critical, task of jointly explaining the equity return and risk premium dynamics in a coherent general equilibrium setting. For concreteness, we initially explore a couple of specific models featuring a representative agent with Epstein-Zin preferences exposed to risks in real consumption growth, namely Wachter (2013) and Drechsler and Yaron (2011).

In the one-factor model of Wachter (2013), the consumption growth is subject to infrequent, but large, negative jumps (rare disasters) with a time-varying arrival rate, resembling the mechanism in Gabaix (2012).²⁹ This type of equilibrium model can account for many critical empirical features such as the correlation between volatility and jump risks, the time-varying jump arrival as well as the ability of the market variance risk premium to predict

²⁹These papers generalize work by Barro (2006) and Barro and Ursua (2008) in which rare disasters are i.i.d.

future equity excess returns.

The model of Drechsler and Yaron (2011) specifies consumption growth as conditionally
945 Gaussian with a time-varying conditional mean (long-run risk) and conditional volatility.³⁰
The system has three factors, with one driving the conditional mean and two governing the
conditional volatility of consumption growth.³¹ Drechsler and Yaron (2011) show that the
time-varying jump intensity – in turn governed by the volatility state – explains a significant
part of the predictability in the variance risk premia of future excess returns.

950 Figures 9 and 10 summarize the findings from predictive regressions for future volatility
and jump risks as well as equity and variance risk premia in the models of Wachter (2013)
and Drechsler and Yaron (2011), using the concurrent level of the relevant state variables
in each model as predictors. Not surprisingly, given the one-factor structure, the Wachter
(2013) model faces some challenges in accommodating the evidence laid out in Figures 7 and
955 8. Importantly for our analysis, the predictability of future excess returns and variance risk
premia is linked closely to the predictability of the future return variation, and the underlying
pattern of significance is identical in all cases (flat line), and the degree of explanatory power
rises roughly linearly with maturity. Compared to Figure 7, the predictability in the Wachter
(2013) model is inverted, as the return variation is forecast with relatively higher precision
960 over long rather than short horizons. Furthermore, the explanatory power is uniformly too
low. Likewise, referencing Figure 8, the model fails to capture the degree and pattern of
predictability in the excess returns and variance risk premium.³²

³⁰This model builds on Eraker and Shaliastovich (2008) and generalizes many prior models in which consumption growth contains a small predictable persistent component, including the original work of Bansal and Yaron (2004).

³¹One of the state variables that we label volatility factors directly controls the conditional variance of consumption growth, while the other captures the variation in the long run variance of consumption growth.

³²A two-factor extension, like in Seo and Wachter (2013), in which rare disaster probability is driven by two factors, can potentially generate dynamic patterns more consistent with the data. However, as we discuss below in more general terms, such an extension will still produce a close link between the predictability of future risks and risk premia unlike what we find in the data.

Turning to Figure 10, it is evident that the more flexible volatility structure of Drechsler and Yaron (2011) is useful in accommodating some of the stylized features of the data. Nonetheless, it is equally clear that the long-run risk factor helps predict neither the future volatility and jump risks nor the equity and variance risk premia. In this structural setting, essentially all predictability stems from the two volatility factors. They provide the channel through which past variance risk premia generate predictable movements in the equity risk premium. Thus, relative to our empirical finding, captured by Figures 7 and 8, this structural model also ties the predictability of future volatility and jump risks too closely to the predictability of the equity and variance risk premia. Equivalently, the structural model implies a tight relationship between the dynamics of the option panel and the return dynamics of the underlying equity market. In contrast, our empirical results based on model (3) document a partial, and critical, decoupling between the factors driving the equity return dynamics and those governing the pricing of risk, and thus the equity and variance risk premia.

There is a fundamental reason for the discrepancy between our empirical findings and the implications of the structural models of Wachter (2013), and its extension in Seo and Wachter (2013), as well as Drechsler and Yaron (2011). Although the models generate risk premia through different channels – the presence of rare disasters and uncertainty about their arrival (Wachter (2013) and Seo and Wachter (2013)) versus long-run risk and stochastic volatility in consumption growth (Drechsler and Yaron (2011)) – they share a critical feature in the pricing of jump tail risk. They both imply that the ratio $\frac{\nu_i^Q(dx,dy)}{\nu_i^P(dx,dy)}$ is time-invariant. That is, the risk-neutral jump intensity is proportional to that under the actual probability measure, so the two jump intensities are equivalent in terms of their time variation. Therefore, the jump risk premia are generated by changing the distribution of the jump size only. This implies that the variation in the jump intensity is “inherited” under the equivalent change of measure. Consequently, these equilibrium based pricing kernels cannot “generate” new

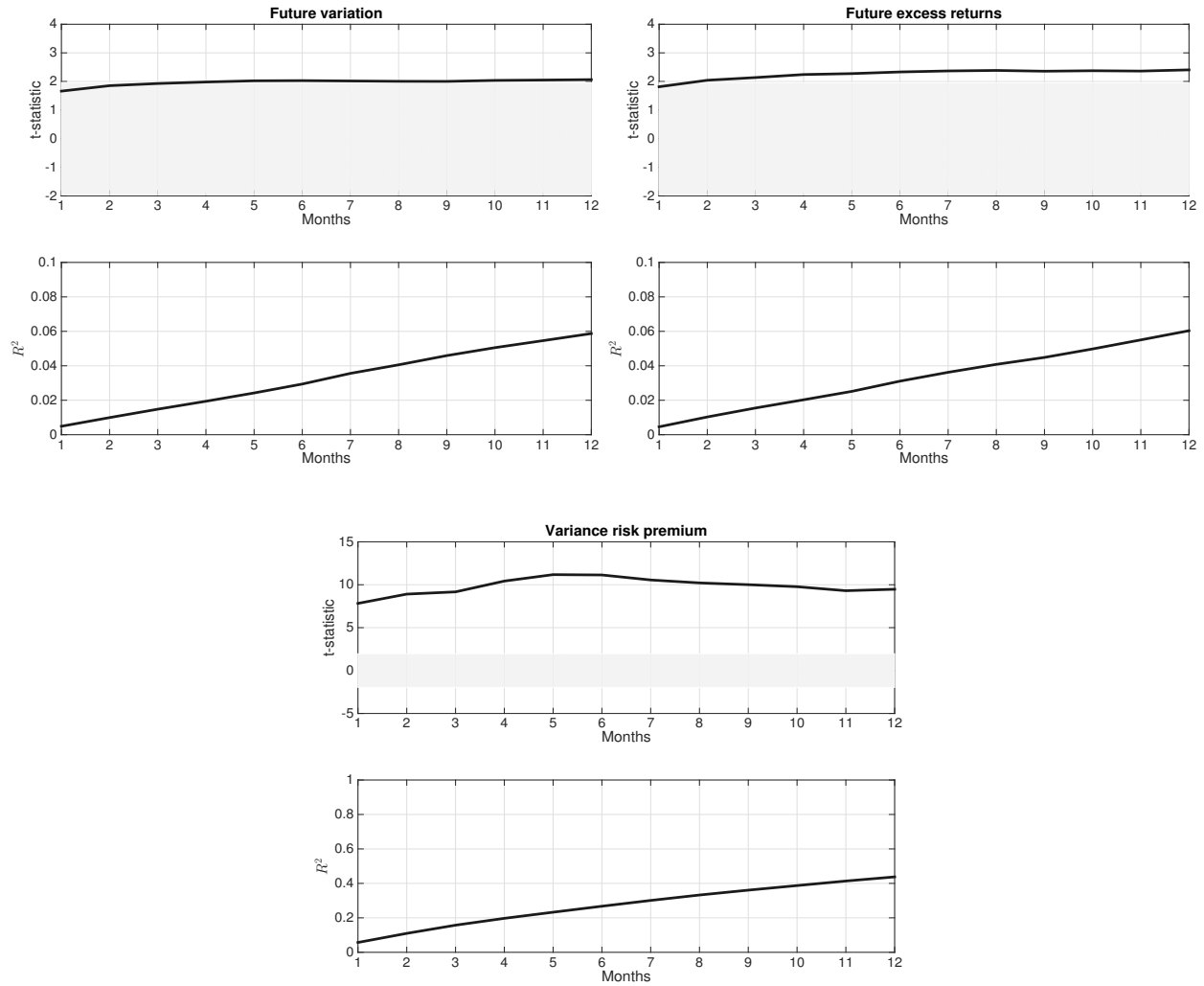


Figure 9: **Predictive Regressions Implied by the Wachter (2013) Structural Model.** The predictive variable is the time-varying intensity of a rare disaster in consumption growth.

state variables in addition to those that drive the fundamental risks in the economy. In turn,
 990 this necessarily generates the tight link between the dynamics of the underlying asset and
 the option surface within these models.

In fact, this tight linkage of the physical and risk-neutral jump intensities is operative for a wide class of popular structural models with representative agents having Epstein-Zin preferences. The part of the density $\frac{dQ}{dP}$ due to the change of the jump measure is

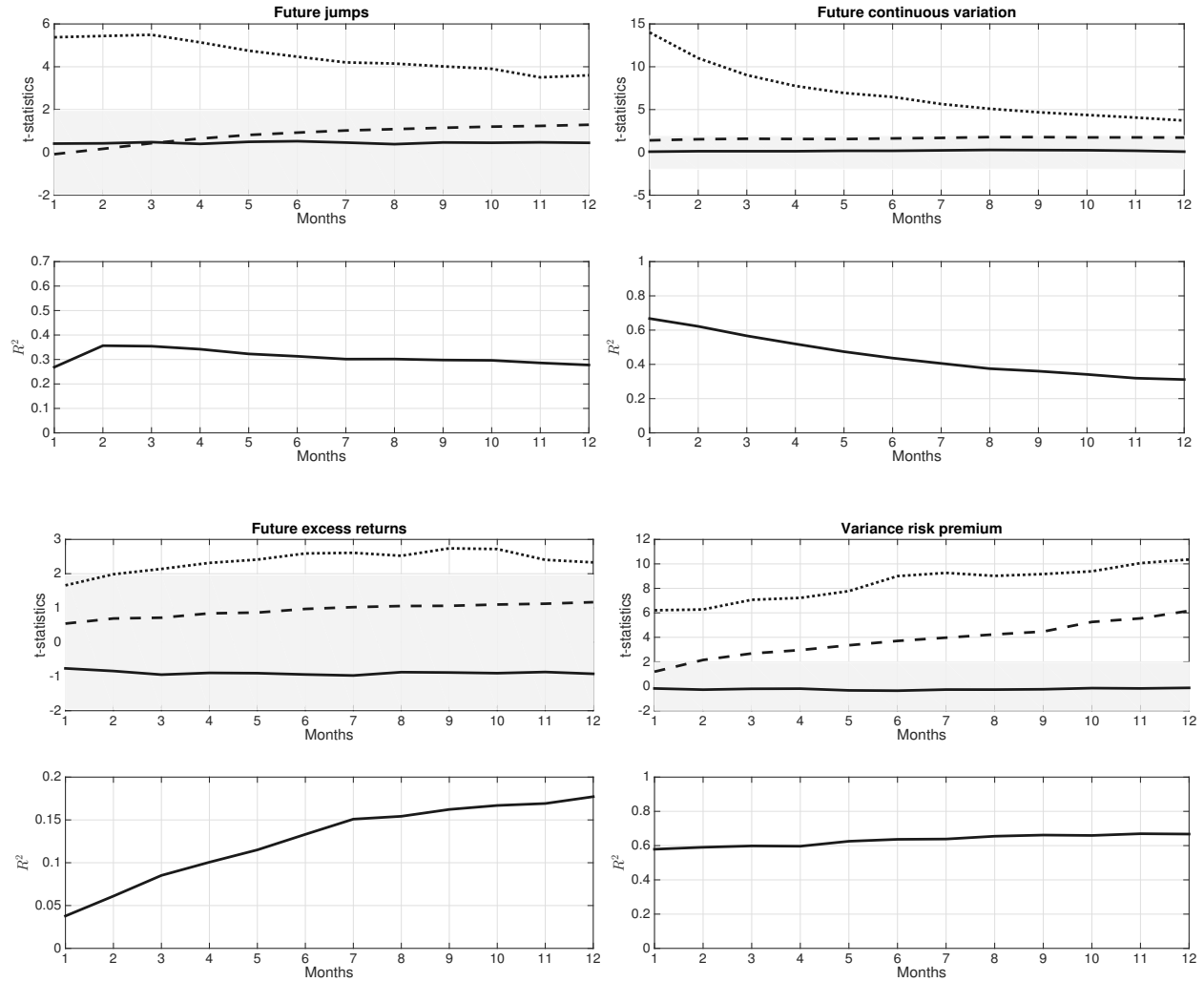


Figure 10: **Predictive Regressions Implied by the Drechsler and Yaron (2011) Structural Model.** The predictive variables are the conditional mean of consumption growth (solid line), stochastic volatility of consumption growth (dotted line) and central tendency of stochastic volatility (dashed line). The dashed lines in the R^2 plots correspond to constrained regressions including only the volatility state variables.

995 characterized by,

$$\mathcal{E} \left(\int_0^t \int_{\mathbb{R}^n} (Y(\omega, s, \mathbf{x}) - 1) \tilde{\mu}^{\mathbb{P}}(ds, d\mathbf{x}) \right), \quad (18)$$

where the jump component of the state vector in the economy under the \mathbb{P} probability measure is given as a (multivariate) integral of the form $\int_0^t \int_{\mathbb{R}^n} \mathbf{x} \tilde{\mu}^{\mathbb{P}}(ds, d\mathbf{x})$; $Y(\omega, t, \mathbf{x}) =$

$\frac{\nu_t^{\mathbb{Q}}(d\mathbf{x})}{\nu_t^{\mathbb{P}}(d\mathbf{x})}$ is the measure change for the jump intensity, and \mathcal{E} is the Doleans-Dade exponential.³³

In general, $Y(\omega, t, \mathbf{x})$ will be stochastic. However, within an equilibrium setting, stipulating
1000 an affine dynamics for the fundamentals along with a representative agent with Epstein-Zin
preferences generates the restriction that the expression in equation (18) is exponentially
affine in the state vector, see, e.g., equation (2.22) of Eraker and Shaliastovich (2008). In
turn, this implies that $Y(\omega, s, \mathbf{x})$ must be non-random and time-invariant, i.e., depend only
on \mathbf{x} .³⁴ Hence, the equilibrium implied statistical and risk-neutral intensities of the price
1005 and volatility jumps (which are mixtures of the jumps in the state variables driving the
fundamentals in the equilibrium model) will be affine functions of the *same* state vector.³⁵ In
contrast, for our extended three-factor model, in which $\nu_t^{\mathbb{P}}(\cdot)$ loads, at most, very marginally
on U_{t-} , there is a natural wedge between the time variation in statistical and risk-neutral
jump intensities.

1010 There are several ways in which the link between the asset and option price dynamics may
be relaxed within a representative agent equilibrium setting to potentially account for our
empirical evidence. They all involve generalizing the preferences in some form. One approach
is to allow the representative agent's coefficient of risk aversion to vary over time. Du (2010)
proposes a generalization of a habit formation model in which consumption growth is i.i.d.
1015 with rare jumps, building on the equilibrium models of Campbell and Cochrane (1999) and
Barro (2006). In this model, and consistent with our findings, there is a wedge between
the time-variation of the \mathbb{P} and \mathbb{Q} jump intensities of the market return distribution. The
nonlinearity of the pricing kernel will amplify the effect of time-varying risk-aversion on the

³³For the expression in (18) and the definition of the Doleans-Dade exponential, see Jacod and Shiryaev (2003), Corollary III.5.22 and I.4.59, respectively.

³⁴The restriction on $Y(\omega, s, \mathbf{x})$ is actually stronger. In the equilibrium model, $Y(\omega, s, \mathbf{x})$ is an exponential function of jump size, see Theorem 1 of Eraker and Shaliastovich (2008). Hence, the jump measure change is implemented by exponential tilting (in Laplace transform space), with the degree of tilting determined by the preference parameters of the representative agent.

³⁵In the models of Wachter (2013), Seo and Wachter (2013) and Drechsler and Yaron (2011), the jump intensities are even more tightly connected, as they are directly proportional.

risk-neutral jump intensity relative to the statistical one. Note that the risk-neutral jump
1020 intensity is nonlinearly related with volatility in this setting, and our U factor will naturally
serve as a proxy for such nonlinearities. Nevertheless, it remains an open question whether
a model with external habit formation can decouple the option and asset price dynamics in
a manner reminiscent of our empirical findings. It is also unclear whether the frequency and
intensity of stock market jumps can be mapped into corresponding jumps in the consumption
1025 growth rate as implied by this model of habit formation.

A second approach to relax the link between the option and asset price dynamics is to
recognize that agents do not directly observe the state vector and therefore need to filter
the states from observables. The absence of perfect information plus aversion to ambiguity
(particularly about extreme negative risks), like in Hansen and Sargent (2008), or lack of
1030 confidence in the estimate of the state vector, like in Bansal and Shaliastovich (2010), can
make investors appear more risk averse than they would be in a perfect information setting.
The key question is whether the ambiguity aversion or confidence risk variation can generate
the required gap between the dynamics of the statistical and risk-neutral jump intensities.³⁶
For example, the excessively tight link between the jump intensity under \mathbb{P} and \mathbb{Q} remains
1035 within the generalization of the Drechsler and Yaron (2011) model, developed by Drechsler
(2013), in which agents are ambiguous about part of the dynamics, including the jumps
in the conditional mean and variance of consumption growth. The representative agent's
ambiguity drives an additional wedge between fundamental risks and asset prices and helps
explain why variance risk premia have superior predictive power, relative to volatility itself,
1040 for future returns. Nonetheless, the linearity of the pricing kernel with respect to the state
vector implies that no new state variable is “generated” going from \mathbb{P} to \mathbb{Q} , thus ultimately
rendering the model predictions incompatible with our empirical findings.

³⁶Recall that, according to the estimates for (3), U does not covary perfectly with stochastic volatility.

Moving beyond the strict representative agent framework, parts of the literature has also considered the potential impact of the intermediary sector for the pricing of derivative securities, particularly following crises; see, e.g., Bates (2003), Hu et al. (2013) and Chen et al. (2014). The main intuition is that major financial shocks may impose losses on market makers and reduce their effective risk bearing capacity. Can we explain the wedge between the factors driving the risks and the risk premia with the health of the financial sector? To informally explore this question, we now relate our U factor to standard measures viewed as proxies for stress in the financial sector. In particular, we incorporate the noise (liquidity) measure of Hu et al. (2013), the 3-month LIBOR minus Treasury (TED) spread, and the default spread defined as the difference between Moodys BAA and AAA bond yield indices (DFSPRD), while also controlling explicitly for volatility. In Table 8, we report the related regression results.

Interestingly, we find the noise factor of Hu et al. (2013) to be quite strongly correlated with our U factor, even after controlling for volatility. While the default spread also has relatively good explanatory power, it is highly correlated with the noise factor, and the individual t-statistics drop substantially when all the variables are included in the (multivariate) regression reported in the last column. Finally, compared to the other factors, the TED spread plays a minimal role. Overall, we conclude that the critical component of U , not correlated with volatility, arguably is associated with proxies for stress in the financial sector. Hence, our procedure, extracting risk premium information directly from the option panel, generates evidence that qualitatively conforms with prior observations in the literature. We leave further explorations along these lines to future work.

8. Conclusion

We document that the standard exponentially-affine jump-diffusive specifications used in the empirical option pricing literature are incapable of fitting critical features of the option

Constant	2.233	0.941	2.632	-0.854	0.976	0.296
	(9.279)	(5.599)	(10.071)	(-0.854)	(5.222)	(1.016)
V	60.834				20.255	19.057
	(6.204)				(2.192)	(2.480)
Noise Fct		0.907			0.727	0.618
		(20.679)			(10.466)	(6.721)
TED			2.279			-1.043
			(4.357)			(-2.960)
DFSPRD				4.616		1.593
				(17.407)		(4.117)
$R^2(\%)$	0.349	0.487	0.094	0.437	0.506	0.549

Table 8: **U factor and the health of the financial sector.** Univariate and multivariate regressions of the U factor on volatility and variables that proxy for the health of the financial sector (t-statistics in parenthesis). V is the variance extracted from the time-series of options panels, *Noise Factor* refers to the liquidity factor proposed by Hu et al. (2013); TED is the spread between the 3-month LIBOR and the Treasury yield; DFSPRD is the difference between BAA and AAA Moodys bond yield indices.

surface dynamics for the S&P 500 index, especially in scenarios involving significant shifts in the volatility smirk. We extend the risk-neutral volatility model to include a separate state variable which is crucial in capturing the time variation of priced downside tail risk. This new factor has no incremental explanatory power, beyond the traditional volatility factors, for the future evolution of volatility and jump risks. On the other hand, relative to the volatility components, the new factor provides critical, and superior, information for the time variation in the equity and variance risk premia.

Our findings demonstrate that the pricing in the option market is closely integrated with the underlying asset market. Moreover, the option panel embodies critical information regarding equity risk pricing that cannot be extracted directly from the underlying asset price dynamics. The wedge between the two probability measures arises primarily from the varying degree of compensation for downward tail jump risk. Our results suggest that time-varying risk aversion and/or ambiguity aversion, driven in part by the presence of large shocks, must be incorporated into structural asset pricing models if they are to explain the joint dynamics of the equity and option markets.

Appendix A. Nonparametric High Frequency Measures

For ease of notation we normalize the time unit to be a day. Each day is then divided into
 1085 a trading and a non-trading part and by convention a day starts with the close of trading on
 the previous day and ends at the closing of the following day trading period. The resulting
 daily interval $[t - 1, t]$ is divided into $[t - 1, t - 1 + \pi]$ overnight period and $[t - 1 + \pi, t]$
 active part of the trading day. Over the trading part, we observe the futures price at $n + 1$
 equidistant times, resulting in n intraday increments, each over a time interval of length
 1090 $\Delta_n \equiv \frac{1-\pi}{n}$. The intraday increments are given by $\Delta_i^{n,t} f = f_{t-1+\pi+i\Delta_n} - f_{t-1+\pi+(i-1)\Delta_n}$ for
 $i = 1, \dots, n$ and $t = 1, \dots, T$.

$\widehat{V}_t^{(n,m_n)}$ is a nonparametric estimator of the diffusive return variation constructed from
 the intraday record of the log-futures price of the underlying asset, f , as follows,

$$\widehat{V}_t^{(n,m_n)} = \frac{n}{m_n} \sum_{i=n-m_n+1}^n (\Delta_i^{n,t} f)^2 1_{\{|\Delta_i^{n,t} f| \leq v \Delta_n^\varpi\}}, \quad (\text{A.1})$$

where $v > 0$, $\varpi \in (0, 1/2)$, and m_n denotes some deterministic sequence. For $m_n/n \rightarrow 0$,
 1095 $\widehat{V}_t^{(n,m_n)}$ is a consistent estimator of the spot variance at t and corresponds to the truncated
 variation (Mancini (2009)) computed over an asymptotically shrinking fraction of the day
 just prior to the option quote. In our implementation, we sample every minute over a 6.75
 hours trading day, excluding the initial five minutes, resulting in $n = 400$. We employ
 $m_n = 300$ for $\widehat{V}_t^{(n,m_n)}$ in (9).

1100 Similarly, we introduce the following measures of jump and variance risks for our analysis
 in Section 7,

$$\begin{cases} \widehat{LT}_{t,t+\tau}^{K,i} = \sum_{s=t+1}^{t+\tau} \sum_{i=1}^n 1_{\{\Delta_i^{n,s} f < -K \vee (v \Delta_n^\varpi)\}}, \\ \widehat{RT}_{t,t+\tau}^{K,i} = \sum_{s=t+1}^{t+\tau} \sum_{i=1}^n 1_{\{\Delta_i^{n,t} f > K \vee (v \Delta_n^\varpi)\}}, \end{cases} \quad (\text{A.2})$$

$$\widehat{QV}_{t,t+\tau}^i = \sum_{s=t+1}^{t+\tau} \sum_{i=1}^n |\Delta_i^{n,t} f|^2, \quad \widehat{QV}_{t,t+\tau}^{c,i} = \sum_{s=t+1}^{t+\tau} \sum_{i=1}^n |\Delta_i^{n,t} f|^2 1_{\{|\Delta_i^{n,t} f| \leq v \Delta_n^{\varpi}\}}, \quad (\text{A.3})$$

where recall K is the constant jump threshold given in (16).

Under general conditions, see, e.g., Jacod (2008),

$$\widehat{LT}_{t,t+\tau}^{K,i} \xrightarrow{\mathbb{P}} LT_{t,t+\tau}^{K,i}, \quad \widehat{RT}_{t,t+\tau}^{K,i} \xrightarrow{\mathbb{P}} RT_{t,t+\tau}^{K,i}, \quad \widehat{QV}_{t,t+\tau}^i \xrightarrow{\mathbb{P}} QV_{t,t+\tau}^i, \quad \widehat{QV}_{t,t+\tau}^{c,i} \xrightarrow{\mathbb{P}} QV_{t,t+\tau}^{c,i}. \quad (\text{A.4})$$

1105 For the overnight periods within $[t, t + \tau]$, we cannot separate the diffusive volatility from jumps, and we simply estimate the total (realized) overnight variance via,

$$\widehat{QV}_{t,t+\tau}^o = \sum_{s=t+1}^{t+\tau} (f_{s-1+\pi} - f_{s-1})^2. \quad (\text{A.5})$$

Our estimate for the total variation, $QV_{t,t+\tau}$, is then given by $\widehat{QV}_{t,t+\tau} = \widehat{QV}_{t,t+\tau}^i + \widehat{QV}_{t,t+\tau}^o$.

Theoretically, for all of the above estimators, any $v > 0$ and $\varpi \in (0, 1/2)$ will work.

1110 We fix $\varpi = 0.49$. The computation of v is more involved and takes into account the fact that volatility varies over time and displays a strong diurnal pattern over the trading day. To account for the latter, we estimate, nonparametrically, a time-of-day factor TOD_i , $i = 1, \dots, n$,

$$TOD_i = NOI_i \frac{\sum_{t=1}^T (\Delta_i^{n,t} f)^2 1_{\{|\Delta_i^{n,t} f| \leq v \Delta_n^{0.49}\}}}{\sum_{t=1}^T \sum_{j=1}^n (\Delta_j^{n,t} f)^2 1_{\{|\Delta_j^{n,t} f| \leq v \Delta_n^{0.49}\}}}, \quad (\text{A.6})$$

where \bar{v} is

$$\bar{v} = 3 \sqrt{\frac{\pi}{2}} \sqrt{\frac{1}{T} \sum_{t=1}^T \sum_{i=2}^n |\Delta_{i-1}^{n,t} f| |\Delta_i^{n,t} f|}, \quad (\text{A.7})$$

1115 and the number of increments factor NOI_i is defined as

$$NOI_i = \frac{\sum_{t=1}^T \sum_{j=1}^n 1_{\{|\Delta_j^{n,t} f| \leq \bar{v} \Delta_n^{0.49}\}}}{\sum_{t=1}^T 1_{\{|\Delta_i^{n,t} f| \leq \bar{v} \Delta_n^{0.49}\}}}. \quad (\text{A.8})$$

The latter ensures that the numerator and denominator in (A.6) are given in identical units. The truncation level \bar{v} is based on the average in-sample volatility obtained from the bipower variation measure of Barndorff-Nielsen and Shephard (2004). The TOD factor is depicted in Figure A.11.

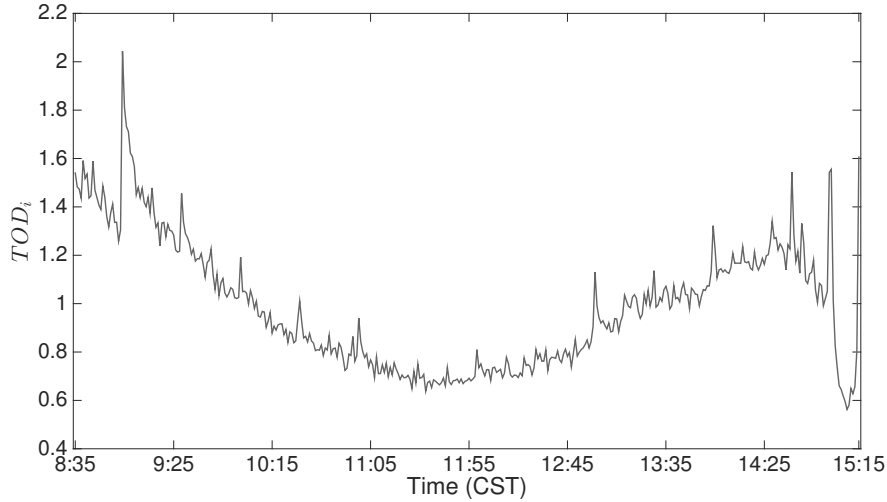


Figure A.11: Time-of-day factor.

1120 To account for time-varying volatility across days, we use the estimated continuous component of volatility for the previous day (for the first day we use \bar{v}). Finally, our time-varying threshold is

$$v_{t,i} = 3 \sqrt{\frac{\widehat{V}_{t-1}^{n,n}}{1 - \widehat{\pi}}} \times TOD_i \times \Delta_n^{0.49}, \quad (\text{A.9})$$

where $\widehat{\pi}$ is given by,

$$\widehat{\pi} = \frac{\sum_{t=1}^T (f_{t+\pi} - f_t)^2}{\sum_{t=1}^T (f_{t+1} - f_t)^2}. \quad (\text{A.10})$$

Appendix B. Linking Risks and Risk Premia with their Feasible Counterparts

1125 From the properties of the compensator for a jump measure, we have,

$$\begin{aligned} LT_{t,t+\tau}^K &= \int_t^{t+\tau} \int_{\mathbb{R}^2} 1_{\{x \leq -K\}} \nu_s^{\mathbb{P}}(dx, dy) ds + \epsilon_{t,t+\tau}^L, & \mathbb{E}_t^{\mathbb{P}}(\epsilon_{t,t+\tau}^L) &= 0, \\ RT_{t,t+\tau}^K &= \int_t^{t+\tau} \int_{\mathbb{R}^2} 1_{\{x \geq K\}} \nu_s^{\mathbb{P}}(dx, dy) ds + \epsilon_{t,t+\tau}^R, & \mathbb{E}_t^{\mathbb{P}}(\epsilon_{t,t+\tau}^R) &= 0. \end{aligned} \quad (\text{B.1})$$

Hence, up to martingale difference sequences, $LT_{t,t+\tau}^K$ and $RT_{t,t+\tau}^K$ measure the \mathbb{P} jump intensity of “large” jumps.³⁷

Turning towards the equity and variance risk premia, we first note that, from an application of Itô formula, $\log(X_t)$ has the following representation under \mathbb{P} ,

$$d \log(X_t) = [\alpha_t - q_t^{\mathbb{P}}] dt + \sqrt{V_{1,t}} dW_{1,t}^{\mathbb{P}} + \sqrt{V_{2,t}} dW_{2,t}^{\mathbb{P}} + \int_{\mathbb{R}^2} x \widetilde{\mu}^{\mathbb{P}}(dt, dx, dy), \quad (\text{B.2})$$

1130 where $q_t^{\mathbb{P}} = \frac{1}{2}V_{1,t} + \frac{1}{2}V_{2,t} + \int_{\mathbb{R}^2} (e^x - 1 - x) \nu_t^{\mathbb{P}}(dx, dy)$, and similarly under \mathbb{Q} with α_t replaced by $r_t - \delta_t$ and all superscripts \mathbb{P} replaced with \mathbb{Q} in the expression above.

Hence, we have the following relations for the feasible measures of the equity and variance risk premia,

$$\begin{aligned} \log\left(\frac{X_{t+\tau}}{X_t}\right) - \frac{1}{\tau} \int_t^{t+\tau} (r_s - \delta_s) ds &= \text{ERP}_t^\tau + \frac{1}{\tau} \mathbb{E}_t^{\mathbb{P}}\left(\int_t^{t+\tau} q_s^{\mathbb{P}} ds\right) + \epsilon_{t,t+\tau}^E, & \mathbb{E}_t^{\mathbb{P}}(\epsilon_{t,t+\tau}^E) &= 0, \\ \widehat{\text{VRP}}_t^\tau &= \frac{1}{\tau} \left[\widehat{QV}_{t,t+\tau} - \mathbb{E}_t^{\mathbb{Q}}(QV_{t,t+\tau}) \right] = \text{VRP}_t^\tau + \epsilon_{t,t+\tau}^V, & \mathbb{E}_t^{\mathbb{P}}(\epsilon_{t,t+\tau}^V) &= 0, \end{aligned} \quad (\text{B.3})$$

³⁷Empirical estimates for the number of “large” negative and positive jumps across our sample are provided in Section C of the Supplementary Appendix.

where $\mathbb{E}_t^{\mathbb{Q}}(QV_{t,t+\tau})$ can be measured in model-free fashion via the VIX index. Equation (B.3) shows that a martingale difference sequence separates $\widehat{\text{VRP}}_t^\tau$ from VRP_t^τ , and, likewise, a martingale difference sequence separates the log excess cum-dividend returns on the underlying asset from the unobservable $\text{ERP}_t^\tau + \frac{1}{\tau} \mathbb{E}_t^{\mathbb{P}} \left(\int_t^{t+\tau} q_s^{\mathbb{P}} ds \right)$. In principle, we can remove the
 1140 term stemming from the convexity adjustment, i.e., $\frac{1}{\tau} \mathbb{E}_t^{\mathbb{P}} \left(\int_t^{t+\tau} q_s^{\mathbb{P}} ds \right)$, via a consistent estimator for $\int_t^{t+\tau} q_s^{\mathbb{P}} ds$ (again up to a martingale difference term) obtained from high-frequency data, e.g.,³⁸

$$\int_t^{t+\tau} \widehat{q}_s^{\mathbb{P}} ds = \sum_{i: \frac{i}{n} \in (t, t+\tau]} \left[\frac{1}{2} |\Delta_i^n f|^2 1_{\{|\Delta_i^n f| \leq v_{t,i}\}} + (e^{\Delta_i^n f} - 1 - \Delta_i^n f) 1_{\{|\Delta_i^n f| > v_{t,i}\}} \right]. \quad (\text{B.4})$$

In practice, this adjustment is minute and the results are virtually unchanged if we implement it.³⁹

1145 References

- Ahn, D., Dittmar, R., Gallant, A., 2002. Quadratic Term Structure Models: Theory and Evidence. *Review of Financial Studies* 15, 243–288.
- Andersen, T. G., Bondarenko, O., Gonzalez-Perez, M. T., 2014. Exploring the Equity-Index Return Dynamics via Corridor Implied Volatility. Working paper, Northwestern University.
- 1150 Andersen, T. G., Fusari, N., Todorov, V., 2013. Parametric Inference and Dynamic State Recovery from Option Panels. Working paper, Northwestern University.
- Andrews, D., 2001. Testing When a Parameter is on the Boundary of the Maintained Hypothesis. *Econometrica* 69, 683–734.

³⁸For the overnight periods we just take one half of the squared return.

³⁹We do not report results adjusting for this term to conserve space. They are available upon request.

- Bai, J., Ng, S., 2002. Determining the Number of Factors in Approximate Factor Models.
1155 *Econometrica* 70, 191–221.
- Bansal, R., Shaliastovich, I., 2010. Confidence Risk and Asset Prices. *American Economic Review* 100, 537–541.
- Bansal, R., Yaron, A., 2004. Risks for the Long Run: A Potential Resolution of Asset Pricing Puzzles. *Journal of Finance* 59, 1481–1509.
- 1160 Barndorff-Nielsen, O. E., Shephard, N., 2004. Power and Bipower Variation with Stochastic Volatility and Jumps. *Journal of Financial Econometrics* 2, 1–37.
- Barro, R., Ursua, J. F., 2008. Macroeconomic Crises since 1870. *Brookings Papers on Economic Activity*, 255–335.
- Barro, R. J., 2006. Rare Disasters and Asset Markets in the Twentieth Century. *Quarterly*
1165 *Journal of Economics* 121, 823–866.
- Bates, D. S., 1991. The Crash of '87 – Was It Expected? The Evidence from Options Markets. *Journal of Finance* 46, 1009–1044.
- Bates, D. S., 2000. Post-'87 Crash Fears in S&P 500 Future Options. *Journal of Econometrics* 94, 181–238.
- 1170 Bates, D. S., 2003. Empirical Option Pricing: A Retrospection. *Journal of Econometrics* 116, 387–404.
- Bates, D. S., 2012. U.S. Stock Market Crash Risk, 1926 - 2010. *Journal of Financial Economics* 105, 229–259.
- Bollerslev, T., Tauchen, G., Zhou, H., 2009. Expected Stock Returns and Variance Risk
1175 Premia. *Review of Financial Studies* 22, 4463–4492.

- Bollerslev, T., Todorov, V., 2011. Tails, Fears and Risk Premia. *Journal of Finance* 66, 2165–2211.
- Bollerslev, T., Todorov, V., 2013. Time Varying Jump Tails. *Journal of Econometrics*, forthcoming.
- 1180 Broadie, M., Chernov, M., Johannes, M., 2007. Specification and Risk Premiums: The Information in S&P 500 Futures Options. *Journal of Finance* 62, 1453–1490.
- Brockwell, P., 2001. Continuous-Time ARMA Processes. In: Shanbhag, D., Rao, C. (Eds.), *Handbook of Statistics*. Vol. 19. North-Holland.
- Campbell, J., Cochrane, J., 1999. By Force of Habit: A Consumption Based Explanation of
1185 Aggregate Stock Market Behavior. *Journal of Political Economy* 107, 205–251.
- Chen, H., Jostlin, S., Ni, S., 2014. Demand for Crash Insurance, Intermediary Constraints, and Stock Return Predictability. Working paper.
- Chernozhukov, V., Hong, H., 2004. Likelihood Estimation and Inference in a Class of Non-regular Econometric Models. *Econometrica* 72, 1445–1480.
- 1190 Christoffersen, P., Heston, S., Jacobs, K., 2009. The Shape and Term Structure of the Index Option Smirk: Why Multifactor Stochastic Volatility Models Work so Well? *Management Science* 55, 1914–1932.
- Christoffersen, P., Jacobs, K., Ornathanalai, C., 2012. Dynamic Jump Intensities and Risk Premiums: Evidence from S&P 500 Returns and Options. *Journal of Financial Economics*
1195 106, 447–472.
- Drechsler, I., 2013. Uncertainty, Time-Varying Fear, and Asset Prices. *Journal of Finance*, forthcoming.

- Drechsler, I., Yaron, A., 2011. What's Vol Got to Do with It? *Review of Financial Studies* 24, 1–45.
- 1200 Du, D., 2010. General Equilibrium Pricing of Options with Habit Formation and Event Risks. *Journal of Financial Economics* 99, 400–426.
- Duffie, D., Filipović, D., Schachermayer, W., 2003. Affine Processes and Applications in Finance. *Annals of Applied Probability* 13(3), 984–1053.
- Duffie, D., Pan, J., Singleton, K., 2000. Transform Analysis and Asset Pricing for Affine
1205 Jump-Diffusions. *Econometrica* 68, 1343–1376.
- Eraker, B., Shaliastovich, I., 2008. An Equilibrium Guide to Designing Affine Pricing Models. *Mathematical Finance* 18, 519–543.
- French, K., Schwert, W., Stambaugh, R., 1987. Expected Stock Returns and Volatility. *Journal of Financial Economics* 19, 3–29.
- 1210 Gabaix, X., 2012. Variable Rare Disasters: An Exactly Solved Framework for Ten Puzzles in Macro-Finance. *Quarterly Journal of Economics* 127, 645–700.
- Glosten, L., Jaganathan, R., Runkle, D., 1993. On the Relation between the Expected Value and the Volatility of the Nominal Excess Return on Stocks. *Journal of Finance* 48, 1779–1801.
- 1215 Hansen, L., Sargent, T., 2008. *Robustness*. Princeton University Press.
- Hu, G., Pan, J., Wang, J., 2013. Noise as Information for Illiquidity. *Journal of Finance* 68, 2223–2772.
- Jacod, J., 2008. Asymptotic Properties of Power Variations and Associated Functionals of Semimartingales. *Stochastic Processes and their Applications* 118, 517–559.

- 1220 Jacod, J., Shiryaev, A. N., 2003. *Limit Theorems For Stochastic Processes*, 2nd Edition. Springer-Verlag, Berlin.
- Johnson, T., 2012. *Equity Risk Premia and the VIX Term Structure*. Working paper, Stanford University.
- Kou, S., 2002. A Jump Diffusion Model for Option Pricing. *Management Science* 48, 1086–
1225 1101.
- Leippold, M., Wu, L., 2002. Asset Pricing under the Quadratic Class. *Journal of Financial and Quantitative Analysis* 37, 271–295.
- Mancini, C., 2009. Non-parametric Threshold Estimation for Models with Stochastic Diffusion Coefficient and Jumps. *Scandinavian Journal of Statistics* 36, 270–296.
- 1230 Merton, R., 1976. Option Pricing when Underlying Asset Returns are Discontinuous. *Journal of Financial Economics* 3, 125–144.
- Santa-Clara, P., Yan, S., 2010. Crashes, Volatility and the Equity Premium: Lessons from S&P 500 Options. *Review of Economics and Statistics* 92, 435–451.
- Santa-Clara, P., Yan, S., 2010. Crashes, Volatility, and the Equity Premium: Lessons from
1235 S&P 500 Options. *Review of Economics and Statistics* 92, 435–451.
- Seo, S., Wachter, J. A., 2013. *Option Prices in a Model with Stochastic Disaster Risk*. Working paper, University of Pennsylvania.
- Wachter, J. A., 2013. Can Time-Varying Risk of Rare Disasters Explain Aggregate Stock Market Volatility? *Journal of Finance* 68, 987–1035.